

<sup>1</sup> Increasing prevalence of plant-fungal symbiosis across two  
<sup>2</sup> centuries of environmental change

<sup>3</sup> Joshua C. Fowler<sup>1,2\*</sup>

Jacob Moutouama<sup>1</sup>

Tom E. X. Miller<sup>1</sup>

<sup>4</sup> 1. Rice University, Department of BioSciences, Houston, Texas 77006; 2. University of Miami,

<sup>5</sup> Department of Biology, Miami, Florida;

<sup>6</sup> \* Corresponding author; e-mail: jcf221@miami.edu.

<sup>7</sup> *Manuscript elements:* Figure 1 - Figure 5, Appendix A (including Figure A1 - Figure A14, Table  
<sup>8</sup> A1, and Supplemental Methods).

<sup>9</sup> *Keywords:* climate change, plant-microbe symbiosis, herbarium, museum specimen, spatially-  
<sup>10</sup> varying coefficients model, *Epichloë*, *Poaceae*.

<sup>11</sup> *Manuscript type:* Research Article.

<sup>12</sup> Prepared using the suggested L<sup>A</sup>T<sub>E</sub>X template for *Am. Nat.*

13

## Abstract

14 Species' distributions and abundances are shifting in response to ongoing global climate change.  
15 Mutualistic microbial symbionts can provide their hosts with protection from environmental  
16 stress that may contribute towards resilient responses to environmental change, however these  
17 changes may also disrupt species interactions and lead to declines in hosts and/or symbionts.  
18 Symbionts preserved within natural history specimens offer a unique opportunity to quantify  
19 changes in microbial symbiosis across broad temporal and spatial scales. We asked how the  
20 prevalence of seed-transmitted fungal symbionts of grasses (*Epichloë* endophytes) have changed  
21 over time in response to climate change, and how these changes vary across host species' ranges.  
22 Specifically, we analyzed 2,346 herbarium specimens of three grass host species (*Agrostis hye-*  
23 *malis*, *Agrostis perennans*, *Elymus virginicus*) collected over the past two centuries (1824 – 2019) for  
24 the presence or absence of *Epichloë* symbiosis. We found that endophytes increased in preva-  
25 lence over the last two centuries from ca. 25% prevalence to ca. 75% prevalence, on average,  
26 across three host species. Changes in seasonal climate drivers were associated with increasing  
27 endophyte prevalence. Notably, increasing precipitation during the peak growing season for  
28 *Agrostis* species and decreasing precipitation for *E. virginicus* were associated with increasing en-  
29 dophyte prevalence. Changes in the variability of precipitation and temperature during off-peak  
30 seasons were also important predictors of increasing endophyte prevalence. Our analysis per-  
31 formed favorably in an out-of-sample predictive test with contemporary survey data, a rare extra  
32 step in collections-based research. However, we identified greater local-scale variability in endo-  
33 phyte prevalence in contemporary data compared to model predictions based on historic data,  
34 suggesting new directions that could improve predictive accuracy. Our results provide novel  
35 evidence for a cryptic biological response to climate change that may contribute to the resilience  
36 of host-microbe symbiosis through context-dependent benefits that confer a fitness advantage to  
37 symbiotic hosts under environmental change.

38 Abstract : 300 words

39

## Introduction

40 Understanding how biotic interactions are altered by global change is a major goal of basic and  
41 applied ecological research (Blois et al., 2013; Gilman et al., 2010). Documented responses to  
42 environmental change, such as shifts in species' distributions (Aitken et al., 2008) and phenology  
43 (Piao et al., 2019), are typically blind to concurrent changes in associated biotic interactions.  
44 Empirically evaluating these biotic changes – whether interacting species shift in tandem with  
45 their partners or not (HilleRisLambers et al., 2013) – is crucial to predicting the reorganization  
46 of Earth's biodiversity under global change. Such evaluations have been limited because few  
47 datasets on species interactions extend over sufficiently long time scales of contemporary climate  
48 change (Poisot et al., 2021).

49 Natural history specimens, which were originally collected to study and preserve taxonomic  
50 diversity, present a unique opportunity to explore long-term changes in ecological interactions  
51 across broad spatial and temporal scales (Meineke et al., 2018). Natural history collections, built  
52 and maintained by the efforts of thousands of scientists, are invaluable time machines, primarily  
53 comprised of physical specimens of organisms along with information about the time and place  
54 of their collection. These specimens often preserve physical legacies of ecological processes and  
55 species' interactions from dynamically changing environments across time and space. For exam-  
56 ple, previous researchers have used plant collections (herbaria) to document shifts in phenology  
57 (Berg et al., 2019; Park et al., 2019; Willis et al., 2017), pollination (Duan et al., 2019; Pauw and  
58 Hawkins, 2011), and herbivory (Meineke et al., 2019) related to anthropogenic climate change.  
59 However, few previous studies have leveraged biological collections to examine climate change-  
60 related shifts in a particularly common type of interaction: microbial symbiosis.

61 Microbial symbionts are common to all macroscopic organisms and can have important ef-  
62 fects on their hosts' survival, growth and reproduction (McFall-Ngai et al., 2013; Rodriguez et al.,  
63 2009). Many microbial symbionts act as mutualists, engaging in reciprocally beneficial interac-  
64 tions with their hosts that can ameliorate environmental stress. For example, bacterial symbionts

65 of insects, such as *Wolbachia*, can improve their hosts' thermal tolerance (Renoz et al., 2019; Truitt  
66 et al., 2019), and arbuscular mycorrhizal fungi, documented in 70-90% of families of land plants  
67 (Parniske, 2008), allow their hosts to persist through drought conditions by improving water and  
68 nutrient uptake (Cheng et al., 2021). On the other hand, changes in the mean and variance of  
69 environmental conditions may disrupt microbial mutualisms by changing the costs and bene-  
70 fits of the interaction for each partner, leading the interaction to deteriorate (Aslan et al., 2013;  
71 Fowler et al., 2024). Coral bleaching (the loss of symbiotic algae) due to temperature stress (Sully  
72 et al., 2019) is perhaps the best known example, but this phenomenon is not unique to corals.  
73 Lichens exposed to elevated temperatures experienced loss of photosynthetic function along with  
74 changes in the composition of their algal symbiont community (Meyer et al., 2022). How com-  
75 monly and under what conditions microbial mutualisms deteriorate or strengthen under climate  
76 change remain unanswered questions (Frederickson, 2017). Previous work suggests that these  
77 alternative responses may depend on the intimacy and specialization of the interaction as well  
78 as the physiological tolerances of the mutualist partners (Rafferty et al., 2015; Toby Kiers et al.,  
79 2010; Warren and Bradford, 2014).

80 Understanding of how microbial symbioses are affected by climate change is additionally  
81 complicated by spatial heterogeneity in the direction and magnitude of environmental change  
82 (IPCC, 2021). Beneficial symbionts are likely able to shield their hosts from environmental stress  
83 in locations that experience a small degree of change, but symbionts in locations that experience  
84 changes of large magnitude may be pushed beyond their physiological limits (Webster et al.,  
85 2008). Additionally, symbionts are often unevenly distributed across their hosts' distribution.  
86 Facultative symbionts may be absent from portions of the host range (Afkhami et al., 2014), and  
87 hosts may engage with a diversity of partners (different symbiont species or locally-adapted  
88 strains) across their environments (Fowler et al., 2023; Fraude et al., 2008; Rolshausen et al., 2018).  
89 Identifying broader spatial trends in symbiont prevalence is therefore an important step in de-  
90 veloping predictions for where to expect changes in the symbiosis in future climates.

91 *Epichloë* fungal endophytes are specialized symbionts of cool-season grasses, which have been

92 documented in ~ 30% of cool-season grass species (Leuchtmann, 1992). They are transmitted  
93 vertically from maternal plants to offspring through seeds. Vertical transmission creates a feed-  
94 back between the fitness of host and symbiont (Douglas, 1998; Fine, 1975; Rudgers et al., 2009).  
95 Over time, endophytes that act as mutualists should rise in prevalence within a host population  
96 (Donald et al., 2021). *Epichloë* are known to improve their hosts' drought tolerance (Decunta  
97 et al., 2021) and protect their hosts against herbivores (Crawford et al., 2010) and pathogens (Xia  
98 et al., 2018) likely through the production of a diverse suite of alkaloids and other secondary  
99 metabolites. The fitness feedback induced by vertical transmission leads to the prediction that  
100 endophyte prevalence should be high in populations where these fitness benefits are most impor-  
101 tant. Previous survey studies of contemporary populations have documented large-scale spatial  
102 patterns in endophyte prevalence structured by environmental gradients (Afkhami, 2012; Bazely  
103 et al., 2007; Granath et al., 2007; Sneck et al., 2017). We predicted that prevalence should track  
104 temporal changes in environmental drivers that elicit strong fitness benefits.

105 Early research on *Epichloë* used herbarium specimens to describe the broad taxonomic di-  
106 versity of host species that harbor these symbionts (White and Cole, 1985), establishing that  
107 endophyte symbiosis could be identified in plant tissue from as early as 1851. However, no  
108 subsequent studies, to our knowledge, have used the vast resources of biological collections to  
109 quantitatively assess spatio-temporal trends in endophyte prevalence and their environmental  
110 correlates. Grasses are commonly collected and identified based on the presence of their re-  
111 productive structures, meaning that preserved specimens typically contain seeds, conveniently  
112 preserving the fungi along with their host plants on herbarium sheets. This creates the oppor-  
113 tunity to leverage the unique spatio-temporal sampling of herbarium collections to examine the  
114 response of the symbiosis to historical climate change. However, the predictive ability derived  
115 from historical analyses is rarely tested against contemporary data (Lee et al., 2024). Critically  
116 evaluating whether insights from historical reconstruction are predictive of variation across con-  
117 temporary populations is a crucial step for the field to move from reading signatures of the past  
118 to forecasting ecological dynamics into the future.

119 In this study, we assessed the long-term responses of endophyte symbiosis to climate change  
120 through the use of herbarium specimens of three North American host grass species (*Agrostis*  
121 *hyemalis*, *Agrostis perennans*, and *Elymus virginicus*). We first addressed questions describing spa-  
122 tial and temporal trends in endophyte prevalence: (i) How has endophyte prevalence changed  
123 over the past two centuries? and (ii) How spatially variable are temporal trends in endophyte  
124 prevalence across eastern North America? We then addressed how climate change may be driv-  
125 ing trends in endophyte prevalence by asking: (iii) What is the relationship between temporal  
126 trends in endophyte prevalence and associated changes in climate drivers? We predicted that  
127 aggregate endophyte prevalence would increase over time in tandem with climate warming, and  
128 that hotspots of endophyte change would correspond spatially to hotspots of climate change.  
129 Finally, we evaluated the performance of models built on data from historic specimens with an  
130 out-of-sample test, using data on endophyte prevalence from contemporary surveys of host pop-  
131 ulations. To answer these questions we examined a total of 2,346 historic specimens collected  
132 across eastern North America between 1824 and 2019, and evaluated model performance against  
133 contemporary surveys comprising 1,442 individuals from 63 populations collected between 2013  
134 and 2020.

## 135 Methods

### 136 Focal species

137 Our surveys focused on three native North American grasses: *Agrostis hyemalis*, *Agrostis peren-*  
138 *nans*, and *Elymus virginicus*. Both *Agrostis* species host *Epichloë amarillans* (Craven et al., 2001;  
139 Leuchtmann et al., 2014), while *Elymus virginicus* typically hosts *Epichloë elymi* (Clay and Schardl,  
140 2002). These C<sub>3</sub> grass species are commonly represented in natural history collections with broad  
141 distributions covering much the eastern United States (Fig. 1). *A. hyemalis* is a small short-lived  
142 perennial species that germinates in spring and typically flowers between March and July (most  
143 common collection month: May). *A. perennans* is of similar stature but is longer lived than

144 *Agrostis hyemalis* and flowers in late summer and early autumn (most common collection month:  
145 *A. perennans* is more sparsely distributed, tending to be found in shadier and more  
146 moist habitats, while *A. hyemalis* is commonly found in open and recently disturbed ground.  
147 Both *Agrostis* species are recorded from throughout the Eastern US, but *A. perennans* has a slightly  
148 more northern distribution, whereas *A. hyemalis* is found rarely as far north as Canada and is  
149 listed as a rare plant in Minnesota. *E. virginicus* is a larger and relatively longer-lived species that  
150 is more broadly distributed than the *Agrostis* species. It begins flowering as early as March or  
151 April but continues throughout the summer (most common collection month: July).

152 *Herbarium surveys*

153 We visited nine herbaria between 2019 and 2022 (see Table A1 for a summary of specimens in-  
154 cluded from each collection). With permission from herbarium staff, we acquired seed samples  
155 from 1135 *A. hyemalis* specimens collected between 1824 and 2019, 357 *A. perennans* specimens  
156 collected between 1863 and 2017, and 854 *E. virginicus* specimens collected between 1839 and  
157 2019 (Fig. 1, Fig. 2A, Fig. A1). We chose our focal species in part because they are commonly  
158 represented in herbarium collections, and produce high numbers of seeds, meaning that small  
159 samples would not diminish the value of the specimens for future studies. We collected up  
160 to 5-10 seeds per specimen after examining the herbarium sheet under a dissecting microscope  
161 to ensure that we collected mature seeds, not florets or unfilled seeds, fit for our purpose of  
162 identifying fungal endophytes with microscopy. We excluded specimens for which information  
163 about the collection location and date were unavailable. Each specimen was assigned geographic  
164 coordinates based on collection information recorded on the herbarium sheet using the geocod-  
165 izing functionality of the ggmap R package (Kahle et al., 2019). Many specimens had digitized  
166 collection information readily available, but for those that did not, we transcribed information  
167 printed on the herbarium sheet. Collections were geo-referenced to the nearest county centroid,  
168 or nearest municipality when that information was available. For fifteen of the oldest specimens,  
169 only information at the state level was available, and so we used the state centroid.

170 After collecting seed samples, we quantified the presence or absence of *Epichloë* fungal hyphae  
171 in each specimen using microscopy. We first softened seeds with a 10% NaOH solution, then  
172 stained the seeds with aniline blue-lactic acid stain and squashed them under a microscope  
173 cover slip. We examined the squashed seeds for the presence of fungal hyphae at 200-400X  
174 magnification (Bacon and White, 2018). On average we scored 4.7 intact seeds per specimen of  
175 *A. hyemalis*, 4.2 seeds per specimen of *A. perennans*, and 3.8 seeds per specimen of *E. virginicus*;  
176 we scored 10,342 seeds in total. . Due to imperfect vertical transmission (Afkhami and Rudgers,  
177 2008), it is possible that symbiotic host-plants produce a mixture of symbiotic and non-symbiotic  
178 seeds. We therefore designated a specimen as endophyte-symbiotic if *Epichloë* hyphae were  
179 observed in one or more of its seeds, or non-symbiotic if *Epichloë* hyphae were observed in none  
180 of its seeds. To capture uncertainty in the endophyte scoring process, we recorded both a "liberal"  
181 and a "conservative" endophyte status for each plant specimen. When we identified potential  
182 endophytes with unusual morphology, low uptake of stain, or a small amount of fungal hyphae  
183 across the scored seeds, we recorded a positive liberal status (more likely to be endophyte-  
184 positive) and a negative conservative status (less likely to be endophyte-positive). 89% of scored  
185 plants had matching liberal and conservative scores, reflecting high confidence in endophyte  
186 status. The following analyses used the liberal status, but we repeated all analyses with the  
187 conservative status which yielded qualitatively similar results (Fig. A8).

188 *Modeling spatial and temporal changes in endophyte prevalence*

189 We assessed spatial and temporal changes in endophyte prevalence across each host distribution,  
190 quantifying the "global" temporal trends aggregated across space, and then examining spatial  
191 heterogeneity in the direction and magnitude of endophyte change (hotspots and coldspots)  
192 across the spatial extent of each host's distribution. To account for the spatial non-independence  
193 of geo-referenced occurrences, we used an approximate Bayesian method, Integrated Nested  
194 Laplace Approximation (INLA), to construct spatio-temporal models of endophyte prevalence.  
195 INLA provides a computationally efficient method of ascertaining parameter posterior distribu-

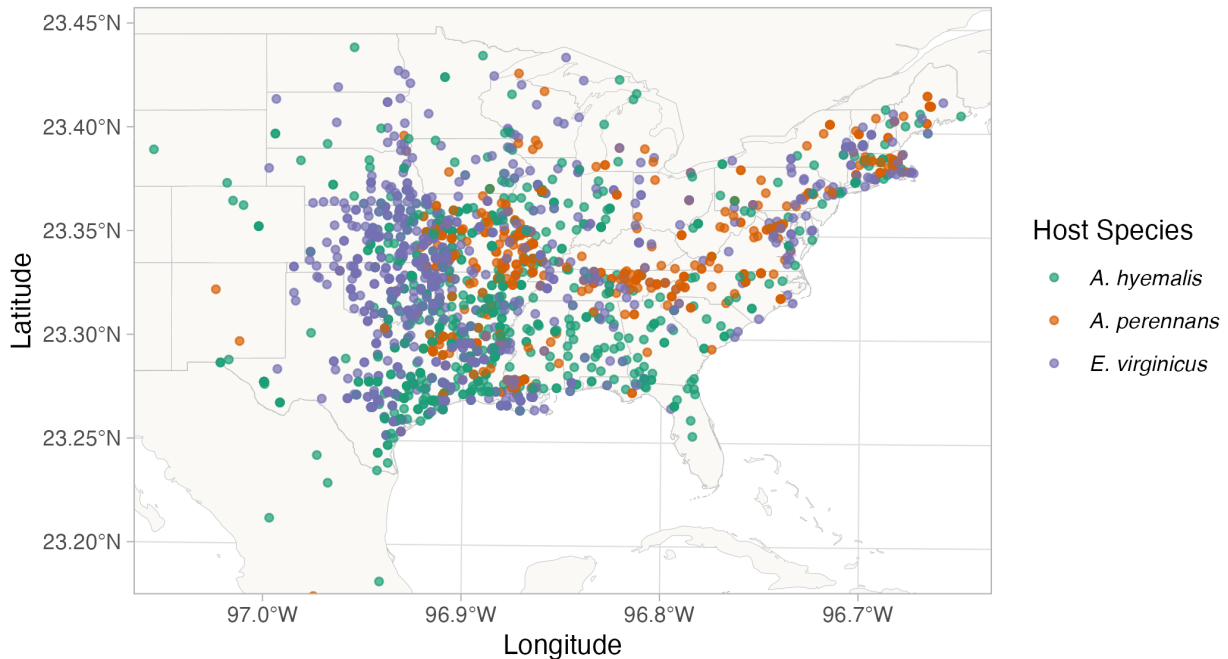


Figure 1: **Collection locations of herbarium specimens sampled for *Epichloë* endophytes.** Specimens span eastern North America from nine herbaria, and are colored by host species.

196 tions for certain models that can be formulated as latent Gaussian Models (Rue et al., 2009).  
197 Many common statistical models, including structured and unstructured mixed-effects models,  
198 can be represented as latent Gaussian Models. We incorporated spatial heterogeneity into this  
199 analysis using spatially-structured intercept and slope parameters implemented as stochastic  
200 partial differential equations (SPDE) to approximate a continuous spatial Gaussian process. This  
201 SPDE approach is a flexible method of smoothing across space while explicitly accounting for  
202 spatial dependence between data-points (Bakka et al., 2018; Lindgren et al., 2011). Fitting models  
203 with structured spatial effects is possible with MCMC sampling but can require long computa-  
204 tion times, making INLA an effective alternative. This approach has been used to model spatial  
205 patterns in flowering phenology (Willems et al., 2022), the abundance of birds (Meehan et al.,  
206 2019) and butterflies (Crossley et al., 2022), the distribution of temperate trees (Engel et al., 2022)  
207 as well as the population dynamics of endangered amphibians (Knapp et al., 2016) and other

208 ecological processes (Beguin et al., 2012).

209 We estimated global and spatially-varying trends in endophyte prevalence using a joint-  
210 likelihood model. For each host species  $h$ , endophyte presence/absence of the  $i^{th}$  specimen ( $P_{h,i}$ )  
211 was modeled as a Bernoulli response variable with expected probability of endophyte occurrence  
212  $\hat{P}_{h,i}$ . We modeled  $\hat{P}_{h,i}$  as a linear function of intercept  $A_h$  and slope  $T_h$  defining the global trend  
213 in endophyte prevalence specific to each host species as well as with spatially-varying intercepts  
214  $\alpha_{h,l_i}$  and slopes  $\tau_{h,l_i}$  associated with location ( $l_i$ , the unique latitude-longitude combination of the  
215  $i^{th}$  observation). The joint-model structure allowed us to “borrow strength” across species in  
216 the estimation of shared variance terms for the spatially-dependent random effect  $\delta_{l_i}$ , intended  
217 to account for residual spatial variation, and  $\chi_{c_i}$  and  $\omega_{s_i}$  i.i.d.-random effects indexed for each  
218 collector identity ( $c_i$ ), and scorer identity ( $s_i$ ) of the  $i^{th}$  specimen.

$$\text{logit}(\hat{P}_{h,i}) = A_h + T_h * \text{year}_i + \alpha_{h,l_i} + \tau_{h,l_i} * \text{year}_i + \delta_{l_i} + \chi_{c_i} + \omega_{s_i} \quad (1)$$

219 By including random effects for collectors and scorers, we accounted for “nuisance” variance  
220 that may bias predictions for changes in endophyte prevalence. Previous work suggests that  
221 behavior of historical botanists may introduce biases into ecological inferences made from historic  
222 collections (Kozlov et al., 2020). Prolific collectors who contribute thousands of specimens may  
223 be more or less likely to collect certain species, or specimens with certain traits (Daru et al., 2018).  
224 Similarly, the process of scoring seeds for hyphae involved several student researchers who, even  
225 with standardized training, may vary in their likelihood of positively identifying *Epichloë*.

226 We performed model fitting using the inlabru R package (Bachl et al., 2019). Global intercept  
227 and slope parameters  $A$ , and  $T$ , were given vague priors. Scorer and collector random effects,  
228  $\chi$  and  $\omega$ , were given penalized complexity priors, with distributions approximating a Normal  
229 distribution with standard deviation of 5. Each spatially-structured parameter depended on a  
230 covariance matrix according to the proximity of each pair of collection locations (Bakka et al.,  
231 2018; Lindgren et al., 2011). The covariance matrix was approximated using a Matérn covariance  
232 function, with each data point assigned a location according to the nodes of a mesh of non-

233 overlapping triangles encompassing the study area (Fig. A2). We assessed model fit with visual  
234 posterior predictive checks (A3) and measurements of AUC (Figs. A4-A5). Priors for the Matérn  
235 covariance function, termed "range" and "variance", define how proximity effects decay with  
236 distance. Results presented in the main text reflect a prior range of 342 kilometers (i.e. a 50%  
237 probability of estimating a range less than 342 kilometers). We tested a range of values (from 68  
238 kilometers to 1714 kilometers) and meshes (presented in the Supporting Methods), finding that  
239 while the magnitude and uncertainty of effects varied, model results were qualitatively similar,  
240 i.e. the same direction of effects across space.

241 *Modeling distributions of host species*

242 Because the herbarium records did not encompass the entirety of these host species' ranges,  
243 we additionally modeled the geographic distribution of each host species to generate realistic  
244 maps on which we could project the predictions of the INLA model. We followed the ODMAP  
245 (overview, data, model, assessment, prediction) protocol (Crossley et al., 2022) (see Supporting  
246 Methods). In short, we used presence-only observations of each host species from Global Bio-  
247 diversity Information Facility (GBIF) between 1990 to 2020. We fit maximum entropy (MaxEnt)  
248 models using the maxent function in the R package dismo (Hijmans et al., 2017) using the same  
249 set of seasonal climate predictors considered above calculated for the 1990-2020 climate normals:  
250 mean and standard deviation of spring, summer, and autumn temperature, and mean and stan-  
251 dard deviation of spring, summer, and autumn cumulative precipitation. We generated 10,000  
252 pseudo-absences as background points, and split the occurrence data into 75% for model train-  
253 ing and 25% for model testing. The performance of models was evaluated with AUC (Jiménez-  
254 Valverde, 2012). We found AUC values of 0.862, 0.838, 0.821 respectively for *Agrostis hyemalis*,  
255 *Agrostis perennans*, and *Elymus virginicus* indicating good model fit to data. To convert the contin-  
256 uous predicted probabilities into binary presence - absence maps on which we projected INLA  
257 predictions, we used the training sensitivity (true positive rate) and specificity threshold (true  
258 negative rate) (Liu et al., 2005).

259

## Assessing the role of climate drivers

260 We assessed how the magnitude of climate change may have driven changes in endophyte prevalence by assessing correlations between changes in climate and changes in endophyte prevalence predicted from our spatial model at evenly spaced pixels across the study area. We first downloaded monthly temperature and precipitation rasters from the PRISM climate group (Daly and Bryant, 2013) covering the time period between 1895 and 2020 using the 'prism' R package (Hart and Bell, 2015). Prism provides reconstructions of historic climate variables across the United States by spatially-interpolating weather station data (Di Luzio et al., 2008). We calculated 30-year climate normals for seasonal mean temperature and cumulative precipitation for the recent (1990 to 2020) and historic (1895 to 1925) periods. We used three four-month seasons within the year (Spring: January, February, March, April; Summer: May, June, July, August; Autumn: September, October, November, December). This division of seasons allowed us to quantify differences in climate associated with the two "cool" seasons, when we expected our focal species to be most biologically active (*A. hyemalis* flowering phenology: spring; *E. virginicus*: spring and summer; *A. perennans*: autumn). In addition to mean climate conditions, environmental variability itself can influence population dynamics (Tuljapurkar, 1982) and changes in variability are a key prediction of climate change models (IPCC, 2021; Stocker et al., 2013). Therefore, we calculated the standard deviation for each annual and seasonal climate driver across each 30-year period. We then took the difference between recent and historic periods for the mean and standard deviation for each climate driver (Figs. A12-A14). All together, we assessed twelve potential climate drivers: the mean and standard deviation of spring, summer, and autumn temperature, as well as the mean and standard deviation of spring, summer, and autumn cumulative precipitation.

281 To evaluate whether areas that have experienced the greatest changes in endophyte prevalence (hotspots of endophyte change) are associated with high degrees of change in climate (hotspots of climate change), we modeled the fitted, spatially-varying slopes of endophyte change through time ( $\tau_{[h]l}$  as a linear function of environmental covariates, with a Gaussian error distri-

285 bution. Data from each host species was analyzed separately. Fitting regressions to many pixels  
286 across the study region risks artificially inflating confidence in our results due to large sample  
287 sizes, and so we performed this analysis using only a random subsample of 250 pixels across the  
288 study region; other sizes of subsample yielded similar results.

289 *Validating model performance with in-sample and out-of-sample tests*

290 We evaluated the predictive ability of the model using both in-sample training data from the  
291 herbarium surveys, and with out-of-sample test data, an important but rarely used strategy in  
292 ecological studies (Lee et al., 2024; Tredennick et al., 2021). We generated out-of-sample test  
293 data from contemporary surveys of endophyte prevalence in natural populations of *A. hyemalis*  
294 and *E. virginicus* in Texas and the southern US. Surveys of *E. virginicus* were conducted in 2013  
295 as described in Sneck et al. (2017), and surveys of *A. hyemalis* took place between 2015 and  
296 2020. Population surveys of *A. hyemalis* were initially designed to cover longitudinal variation  
297 in endophyte prevalence towards its range edge, while surveys of *E. virginicus* were designed to  
298 cover latitudinal variation. In total, we visited 43 populations of *A. hyemalis* and 20 populations  
299 of *E. virginicus* across the south-central US, with emphasis on Texas and neighboring states (Fig  
300 A11). During surveys, we collected seeds from up to 30 individuals per population (average  
301 number of plants sampled per population: 22.9); note that this sampling design provided greater  
302 local depth of information than the herbarium records, where only one plant was sampled at  
303 each locality. We quantified the endophyte status of each individual with staining microscopy  
304 as described for the herbarium surveys (with 5-10 seeds scored per individual), and calculated  
305 the prevalence of endophytes within the population (proportion of plants that were endophyte-  
306 symbiotic). For each population, we compared the observed fraction of endophyte-symbiotic  
307 hosts to the predicted probability of endophyte occurrence  $\hat{P}$  derived from the model for that  
308 location and year. The contemporary survey period (2013-2020) is at the most recent edge of the  
309 time period encompassed by the historical observations used for model fitting.

310

## Results

### 311 *How has endophyte prevalence changed over time?*

312 Across >2300 herbarium specimens dating back to 1824, we found that prevalence of *Epichloë*  
313 endophytes increased over the last two centuries for all three grass host species (Fig. 2). On  
314 average, endophytes of *A. perennans* and *E. virginicus* increased from ~ 40 % to 70% prevalence  
315 across the study region, and *A. hyemalis* increased from ~ 25% to over 50% prevalence. Our  
316 model indicates a high certainty that overall temporal trends are positive across species (99%  
317 probability of a positive overall year slope in *A. hyemalis*, 92% probability of a positive overall  
318 year slope in *A. perennans*, and 91% probability of a positive overall year slope in *E. virginicus*)  
319 (Fig. A6).

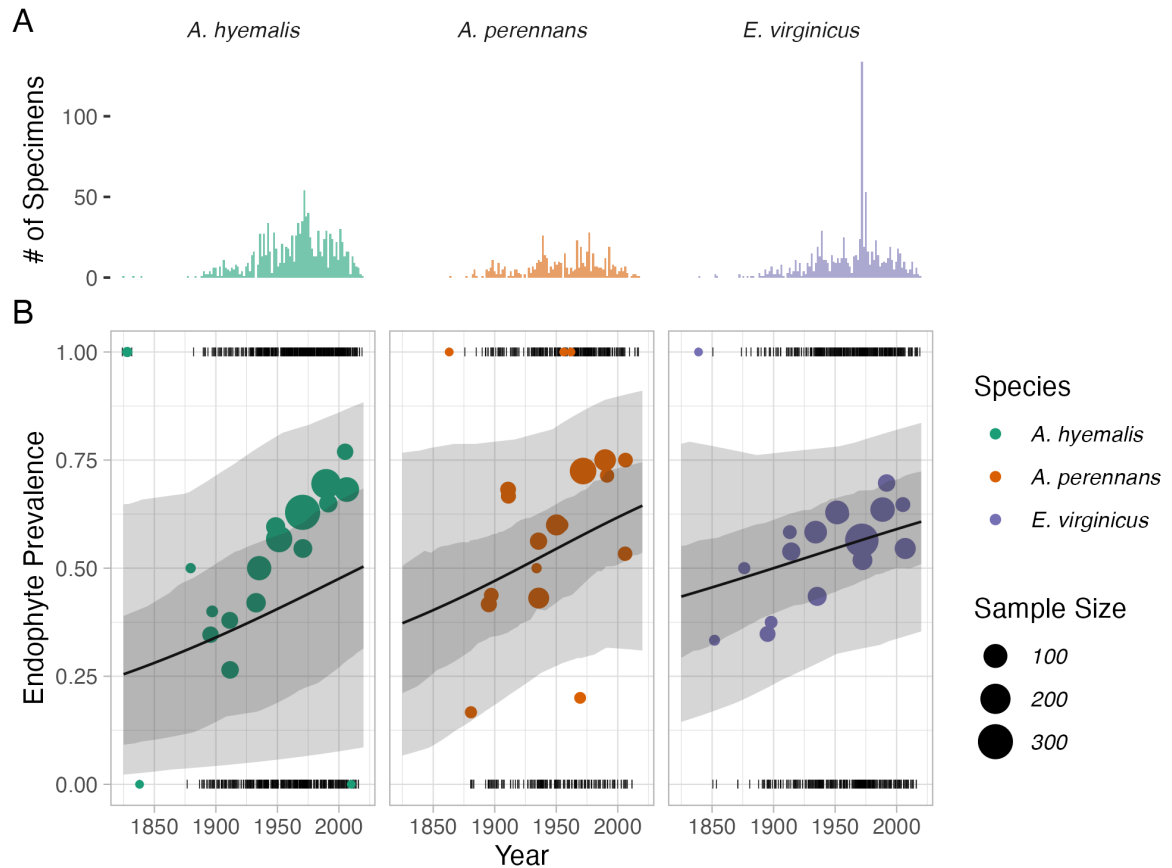


**Figure 2: Temporal trends in endophyte prevalence.** (A) Histograms show the frequency of scored specimens through time for each host species. (B) Lines show predicted mean endophyte prevalence over the study period along with the 50% and 95% CI bands incorporating uncertainty associated with collector and scorer random effects. Colored points are binned means of the observed endophyte presence/absence data (black dashes). Colors represent each host species and point size represents the number of specimens.

320 The model appears to under-predict the observed increase in endophyte prevalence relative  
321 to the data, particularly for *A. hyemalis* (Fig. 2B), but the model is accounting for random effects  
322 and spatial non-independence that are not readily seen in the figure. We found no evidence that  
323 collector biases influenced our results. Collector random effects were consistently small (Fig.  
324 A9), and models fit with and without this random effect provide qualitatively similar results.

325 The identity of individual scorers did contribute to observed patterns in endophyte prevalence.  
326 For example, 3 of the 25 scorers were more consistently likely than average to assign positive  
327 endophyte status, as indicated by 95% credible intervals greater than zero (Fig. A10). It is  
328 difficult to distinguish whether this was driven by true differences in scorers biases during the  
329 seed scoring process or by unintended spatial or temporal clustering of the specimens scored by  
330 each scorer (Clayton et al., 1993; Urdangarin et al., 2023). By under-weighting endophyte-positive  
331 samples that are clustered spatially or by collector or observer, the INLA model is appropriately  
332 accounting for nuisance variables and providing a conservative inference of endophyte change  
333 relative to the raw data.

334 *How spatially variable are temporal trends in endophyte prevalence?*

335 While there was an overall increase in endophyte prevalence, our model revealed hotspots and  
336 coldspots of change across the host species' ranges, which are mapped in Fig. 3 across geo-  
337 graphic ranges predicted by MaxEnt species distribution models. In some regions, posterior  
338 mean estimates of spatially varying temporal trends indicate that *A. hyemalis* and *A. perennans*  
339 experienced increases in prevalence by as much as 2% per year over the study period, while  
340 *E. virginicus* experienced increases up to around 1% per year. Both *Agrostis* species show areas  
341 of strong increase and areas of declining prevalence, while *E. virginicus* had an overall weaker  
342 and geographically more homogeneous increase in endophyte prevalence. Notably, endophytes  
343 increased most strongly towards the western range edge of *A. hyemalis* (Fig. 3A) and across the  
344 northeastern US for *A. perennans* (Fig. 3B). Posterior estimates of uncertainty in spatially varying  
345 slopes indicate that these hotspots of change may have experienced increases of up to 5% per  
346 year while declines in prevalence may be as great as 4% per year for *A. hyemalis* and *A. perennans*.  
347 For *E. virginicus*, uncertainty ranges between 3.5% increases and 2.5% decreases (Fig. A7).

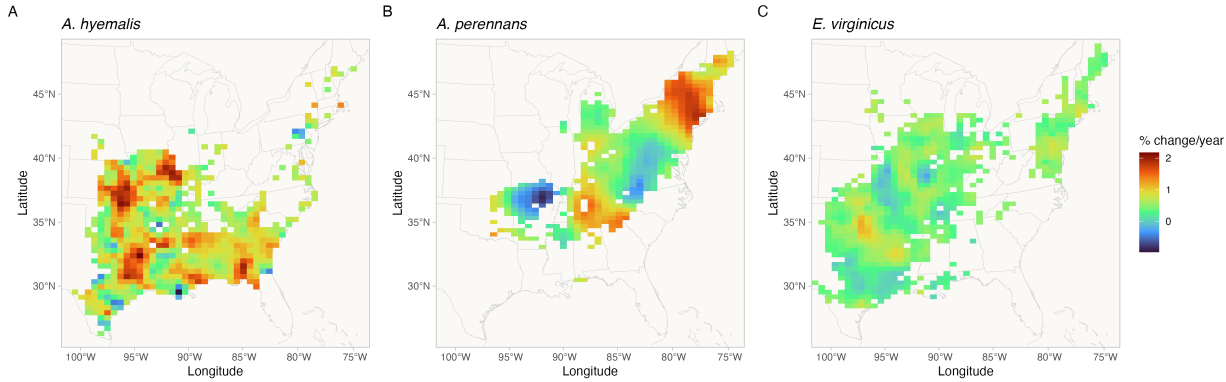


Figure 3: Predicted posterior mean of spatially-varying slopes representing change in endophyte prevalence for each host species. Color indicates the relative change in predicted endophyte prevalence.

348 *What is the relationship between variation in temporal trends in endophyte*

349 *prevalence and changes in climate drivers?*

350 We found that trends in endophyte prevalence were strongly associated with seasonal climate  
351 change drivers (Fig. 4). For the majority of the study region, the climate has become wetter (an  
352 average increase in annual precipitation of 60 mm.) with relatively little temperature warming  
353 (an average increase in annual temperature of 0.02 °C) over the last century (Fig. A12-A14), a con-  
354 sequence of regional variation in global climate change (IPCC, 2021). Within the region, climate  
355 changes were spatially variable; certain locations experienced increases in annual precipitation  
356 as large as 375 mm. or decreases up to 54 mm. across the last century, while annual temper-  
357 ature changes ranged from warming as great as 1.4 °C to cooling by 0.46 °C. Spatially variable  
358 climate trends were predictive of trends in endophyte prevalence. For example, strong increases  
359 in endophyte prevalence for *A. perennans* were most strongly associated with increasing autumn  
360 precipitation and with increasing mean and variability in autumn temperature (greater than 97%  
361 posterior probabilities of positive slopes). For this species, a 1 °C increase in autumn temper-

ature was associated with a 1.07 % increase per year in endophyte prevalence (Fig. 4A) and a 100 mm. increase in precipitation was associated with a 0.8% increase per year in endophyte prevalence (Fig. 4B). This result aligns with the species' autumn active growing season, however other seasonal climate drivers were also associated with increasing endophyte prevalence. In particular, we found cooler and drier springs and cooler summers to be associated with increasing endophyte prevalence (greater than 99% posterior probabilities of negative slopes) however these slopes were generally of smaller magnitude than those for autumn climate drivers.

Changes in endophyte prevalence across the ranges of *A. hyemalis* and *E. virginicus* were less strongly driven by changes in climate. Like *A. perennans*, climate during peak growing season (spring for *A. perennans* and summer for *E. virginicus*) emerged most commonly as drivers of changes in endophyte prevalence. Increases in mean spring precipitation were the strongest predictor of increasing trends in endophyte prevalence for *A. hyemalis* (Fig. 4B) (greater than 99% posterior probability of a positive slope). For this species, an increase of 100 mm. in spring precipitation led to an increase of 0.6% per year in endophyte prevalence. The next greatest slopes were those associated with variability in spring precipitation (greater than 96% posterior probability of a negative slope), as well as in the mean and variability of autumn climate (greater than 98% probability of negative and positive slopes, respectively). Changes in endophyte prevalence in *E. virginicus* were not strongly associated with changes in most climate drivers, but regions with reduced variability in autumn precipitation (Fig. 4B) and with cooler and more variable summer temperatures (Fig. 4A,C) experienced the largest increases in endophyte prevalence. While our analysis identified the importance of these drivers with relatively high certainty (greater than 99% posterior probability of either negative or positive slopes respectively), they translate to less than 0.2% change in endophyte prevalence per year for a change of 100 mm. change in precipitation over the century. Repeating this analysis using all pixels across each species' distribution were qualitatively similar to these results.

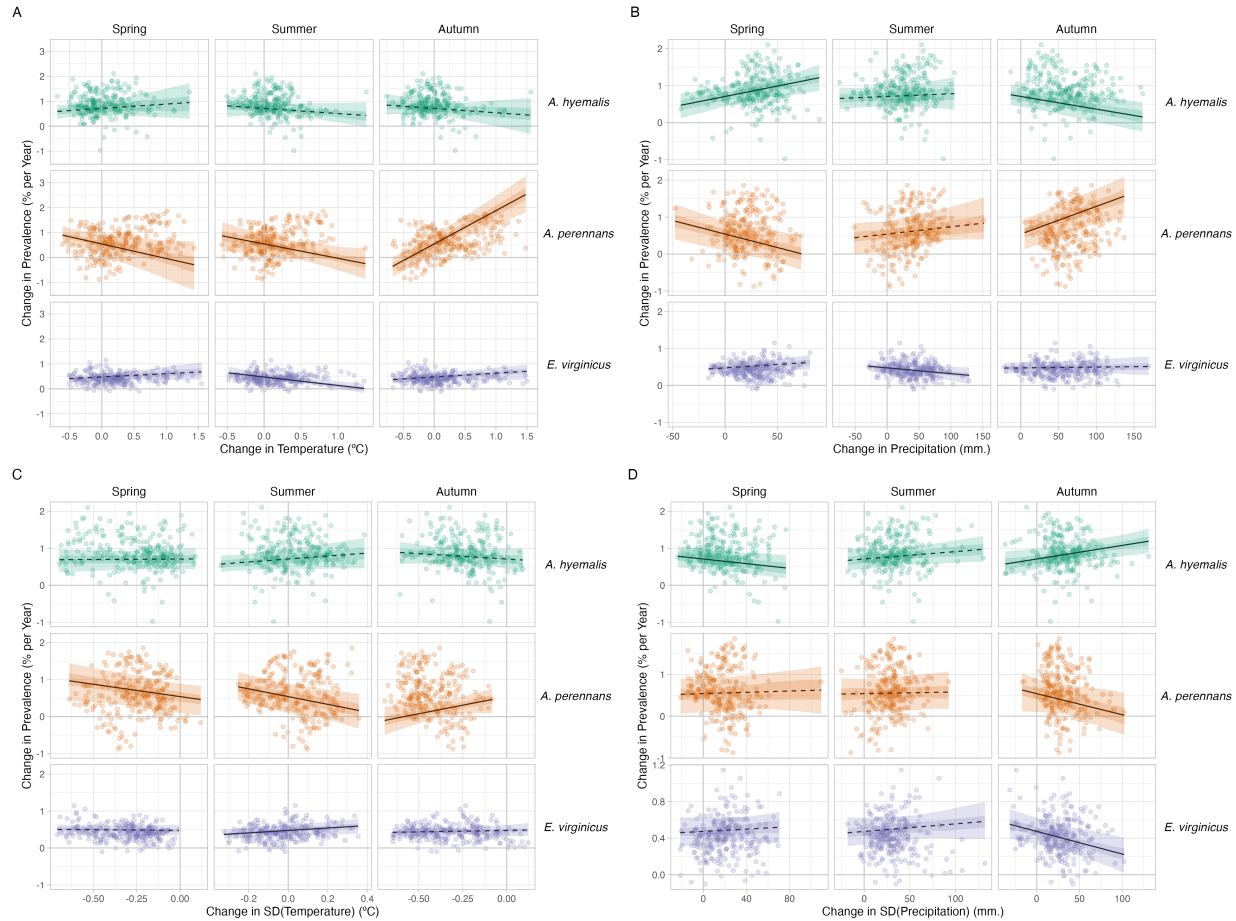


**Figure 4: Relationships between predicted trends in endophyte prevalence and changes in seasonal climate drivers.** Lines show marginal predicted relationship between spatially-varying trends in endophyte prevalence and changes in mean and variability of climate ((A): mean temperature, (B): cumulative precipitation, (C): standard deviation in temperature, (D): standard deviation in precipitation). Confidence bands represent the 50 and 95% CI, colored by host species. Slopes with greater than 95% probability of being either positive or negative are represented as solid lines while those that have less than 95% probability are dashed. Points show 250 randomly sampled pixels across each host's distribution used in model fitting.

387 *Performance on test data*

388 Tests of model's predictive performance as quantified by AUC and by visual posterior predic-  
389 tive checks, indicated good predictive ability. Model performance was similar between historic  
390 herbarium specimens used as training data and the out-of-sample test data from contemporary  
391 surveys (AUC = 0.79 and 0.77 respectively; Fig. A5-A4). The model successfully captured broad  
392 regional trends in endophyte prevalence seen in the contemporary survey data, such as decline  
393 endophyte prevalence in *A. hyemalis* towards western longitudes (Fig. 5A) and northern lati-  
394 tudes (Fig. 5B). However, model predictions for endophyte prevalence exhibited relatively little  
395 local geographic variation, whereas the out-of-sample survey data were maximally variable with  
396 populations spanning 0% to 100% endophyte-symbiotic plants (Fig. 5C). We interpret this to  
397 mean that the model captures coarse-scale spatial and temporal trends reasonably well, but is  
398 not equipped to capture local-scale nuances that generate population-to-population differences.

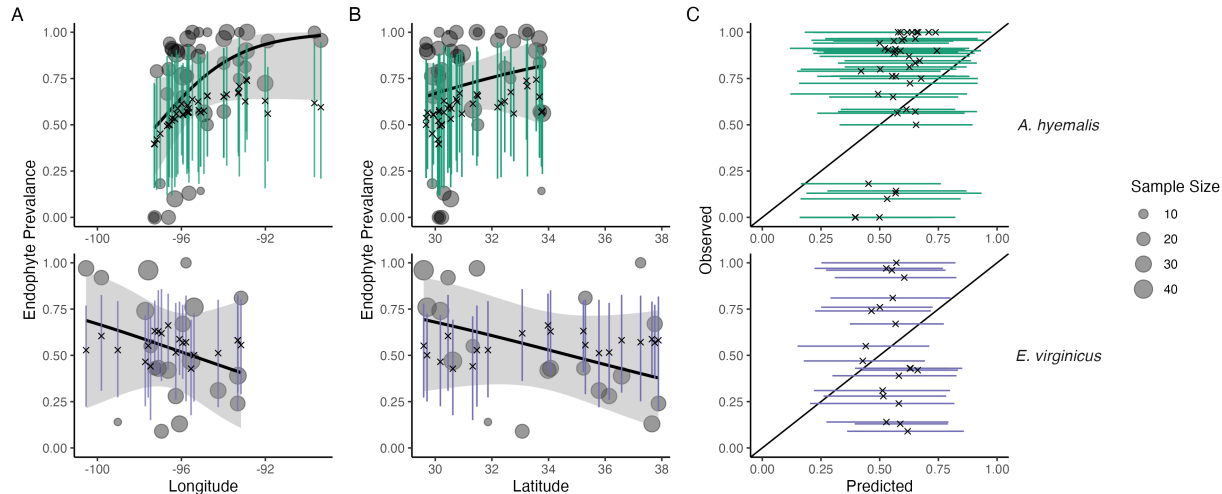


**Figure 5: Predictive performance for contemporary test data.** (A) The model, trained on historic herbarium collection data, performed modestly at predicting prevalence in contemporary population surveys. The model captured regional trends across (A) longitude and (B) latitude. Crosses indicate predicted mean prevalence along with the 95% CI (colored lines) from the herbarium model. Contemporary prevalence is represented by grey points (point size reflects sample size) along with trend lines from generalized linear models (black line and shaded 95% confidence interval). (C) Comparison of observed vs. predicted endophyte prevalence shows that contemporary test data had more variance between populations than contemporary predictions.

## Discussion

Our examination of historic plant specimens revealed cryptic shifts in microbial symbiosis over the last two centuries. For the three host species we examined, there have been strong increases in prevalence of fungal endophytes. We interpret increases in prevalence of *Epichloë*, which are vertically transmitted, as adaptive changes that improve the fitness of their hosts under increasing environmental stress. This interpretation is in line with theory predicting that the positive fitness feedback caused by vertical transmission leads beneficial symbionts to rise in prevalence within a population (Donald et al., 2021; Fine, 1975). We further found that trends in endophyte

407 prevalence varied across the distribution of each species in association with changes in climate  
408 drivers, suggesting that the increases in endophyte prevalence are driven by context-dependent  
409 benefits to hosts that confer resilience under environmental change. Taken together, this suggests  
410 an overall strengthening of host-symbiont mutualism over the last two centuries.

411 Differences across host species underscore that while all of these  $C_3$  grasses share similar  
412 broad-scale distributions, each engages in unique biotic interactions and has unique responses to  
413 environmental drivers. We identified hotspots of change for *A. perennans*, which was the species  
414 that experienced the strongest absolute changes in endophyte prevalence (Fig. 3). Declines of  
415 0.9% per year in the southern portion of its range and increases of up to 2% per year in the  
416 north suggest a potential poleward range shift of endophyte-symbiotic plants (whether the over-  
417 all host distribution is shifting in parallel is an exciting next question). Based on previous work  
418 demonstrating that endophytes can shield their hosts from drought stress (reviewed in Decunta  
419 et al. (2021)), we generally predicted that drought conditions would be a driver of increasing en-  
420 dophyte prevalence. In contrast to this expectation, increasing prevalence for *A. perennans* were  
421 associated with increasing autumn temperature and precipitation (Fig. 4). To our knowledge,  
422 the response of the symbiosis in *A. perennans* to drought has not been examined experimentally,  
423 but in a greenhouse experiment, endophytes had a positive effect on host reproduction under  
424 shaded, low-light conditions (Davitt et al., 2010). Our results also hint that it may be useful to  
425 investigate whether lagged climate effects are important predictors of host fitness in this system  
426 (Evers et al., 2021). Endophyte prevalence of the autumn-flowering *A. perennans* was strongly  
427 linked with decreasing spring precipitation, and that of the spring-flowering *A. hyemalis* was as-  
428 sociated with decreasing autumn precipitation (Fig. 4B). For *A. hyemalis*, endophytes could be  
429 playing a role helping hosts weather autumn-season droughts, which may be an important time  
430 for the species' germination. Previous work has demonstrated drought benefits in a greenhouse  
431 manipulation with this species (Davitt et al., 2011), and early life stages may be particularly vul-  
432 nerable to prolonged droughts. For *E. virginicus*, which experienced the most modest changes  
433 in endophyte prevalence overall (ranging between 1.1% increases and 0.2% decreases), we only

434 found modest associations with changes in climate drivers. Surveys by Sneck et al. (2017), used  
435 as part of the test data in this study, identified a drought index (SPEI) that integrates precipitation  
436 with estimated evapotranspiration as an important predictor of endophyte prevalence. *Epichloë*  
437 endophytes have also been connected to a suite of non-drought related fitness benefits including  
438 herbivore protection (Brem and Leuchtmann, 2001), salinity resistance (Wang et al., 2020), and  
439 mediation of the soil microbiome (Roberts and Ferraro, 2015). These effects are potentially medi-  
440 ated by the diverse bioactive alkaloids and other signaling compounds they produce (Saikkonen  
441 et al., 2013). Increases in symbionts could be explained, at least in part, by these diverse benefits  
442 that may help hosts weather a world made increasingly stressful by changes in climate and other  
443 anthropogenically introduced stressors. While we show consistent increasing trends in preva-  
444 lence between the three species, the mechanisms that explain these changes may be diverse and  
445 idiosyncratic.

446 The combination of a spatially-explicit model and historic herbarium specimens allowed us  
447 to identify regions of both increasing and decreasing endophyte prevalence, however we see  
448 several next steps towards the goal of predicting host and symbiont niche-shifts in response to  
449 future climate change. While the model recreated the large-scale spatial trends observed in con-  
450 temporary population surveys, test data contained more population-to-population variability in  
451 prevalence. Validating our model predictions in this way, a rare extra step in collections-based  
452 studies, allows us to evaluate places to improve the model's out-of-sample predictive ability.  
453 Lack of information on local variability may simply be a feature of data derived from herbarium  
454 specimens. They are samples from local populations, but they are single specimens that are ag-  
455 gregated to derive broad-scale model estimates. This suggests that increasing local replication  
456 should be a factor considered in future collection efforts of natural history specimens, balanced  
457 with the required time and effort. Poor predictive ability at local scales in this grass-endophyte  
458 system is not surprising, as previous studies have found that local variation, even to the scale  
459 of hundreds of meters can structure endophyte-host niches (Kazenel et al., 2015). Other studies  
460 have found factors including land-use history (Vikuk et al., 2019) and the biotic environment,

461 including herbivory (Rudgers et al., 2016), and host genotype Sneck et al. (2017), to be important  
462 predictors of endophyte ecology. An important step would be integrating data from local and  
463 regional scales through modeling to constrain estimates of local and regional variation. Previ-  
464 ous population surveys have found environment-dependent gradients in endophyte prevalence  
465 (Rudgers and Swafford, 2009; Semmarin et al., 2015; Sneck et al., 2017), that may be caused  
466 by symbiont-derived fitness benefits allowing their hosts to persist in environments where they  
467 otherwise could not (Afkhami et al., 2014; Fowler et al., 2023; Kazenel et al., 2015). Predict-  
468 ing future niche-shifts of hosts and symbionts will require considering the coupled dynamics of  
469 host-symbiont dispersal in addition to fitness benefits. For example, transplanting symbiotic and  
470 non-symbiotic plants beyond the range edge of *A. hyemalis* could tell us whether low endophyte  
471 prevalence in that area is a result of environmental conditions that lead the symbiosis to negative  
472 fitness consequences, or is a result of some historical contingency or dispersal limitation that  
473 has thus far limited the presence of symbiotic hosts from a region where they would otherwise  
474 flourish and provide resilience. Incorporating available climatic and soil layers as covariates is  
475 another obvious step that could improve predictions. These steps will bridge gaps that often  
476 exist between large but broad bioclimatic and biodiversity data and small but local data on bi-  
477 otic interactions, and move towards the goal of predicting the dynamics of microbial symbioses  
478 under climate change (Isaac et al., 2020; Miller et al., 2019).

479 Our analysis advances the use of herbarium specimens in global change biology in two ways.  
480 First and foremost, this is the first study to link long-term changes in microbial symbioses to  
481 changes in climate using specimens from natural history collections. The responses of micro-  
482 bial symbioses are a rich target for future studies within museum specimens, particularly those  
483 that take advantage of advances in sequencing technology. While we used relatively coarse  
484 presence/absence data based on fungal morphology, other studies have examined historic plant  
485 microbiomes using molecular sequencing and sophisticated bioinformatics techniques, but these  
486 studies have so far been limited to relatively few specimens at limited spatial extents (Bieker  
487 et al., 2020; Bradshaw et al., 2021; Gross et al., 2021; Heberling and Burke, 2019; Yoshida et al.,

488 2015). Continued advances in capturing historic DNA and in filtering out potential contamina-  
489 tion during specimen storage (Bakker et al., 2020; Daru et al., 2019; Raxworthy and Smith, 2021)  
490 will be imperative in the effort to scale up these efforts. This scaling up will be essential to be  
491 able to quantify changes not just in the prevalence of symbionts, but also in symbionts' intraspe-  
492 cific variation and evolutionary responses to climate change, as well as in changes in the wider  
493 microbial community. Genetic variation in *Epichloë* endophytes, particularly in genes respon-  
494 sible for alkaloid production, produces "chemotypes" with differing benefits for hosts against  
495 insect or mammalian herbivores mediated by environmental conditions (Saikkonen et al., 2013;  
496 Schardl et al., 2012). With improved molecular insights from historic specimens, we could ask  
497 whether the broad increases in endophytes that we have identified reflect selection for particular  
498 chemotypes and how this selection varies across space. Answering these questions as well as  
499 the unknown questions that future researchers may ask also reiterates the value in capturing  
500 meta-information during ongoing digitization efforts at herbaria around the world and during  
501 the accession of newly collected specimens (Edwards et al.; Lendemer et al., 2020). Second, we  
502 accounted for several potential biases in the data observation process that may be common to  
503 many collections-based research questions by using a spatially-explicit random effects model.  
504 Spatial autocorrelation (Willems et al., 2022), potential biases introduced by the sampling habits  
505 of collectors (Daru et al., 2018), and variation between contemporary researchers during the col-  
506 lection of trait data, if not corrected for could lead to over-confident inference about the strength  
507 and direction of historic change (Fig. 2). Previous studies that have quantified the effects of  
508 collector biases typically find them to be small (Davis et al., 2015; Meineke et al., 2019), and we  
509 similarly did not find that collector has a strong effect on the results of our analysis, but that  
510 scorer identity did impact results.

511 Ultimately, a central goal of global change biology is to generate predictive insights into the  
512 future of natural systems on a rapidly changing planet. Beyond host-microbe symbioses, de-  
513 tecting ecological responses to anthropogenic global change and attributing their causes would  
514 inform public policy decision-makers and adaptive management strategies. This survey of his-

515 toric endophyte prevalence is necessarily correlative, yet it serves as a foundation to develop  
516 better predictive models of the response of microbial symbioses to climate change. By compar-  
517 ing detected ecological responses with alternative mechanistic simulations of the past, we could  
518 attribute their cause, in a manner similar to methods from climate science and economics (Car-  
519 leton and Hsiang, 2016; Stott et al., 2010; Trenberth et al., 2015). Combining the insights from  
520 this type of regional-scale survey with field experiments and physiological performance data  
521 could be invaluable to identify mechanisms driving shifts in host-symbiont dynamics. Evidence  
522 is strong that certain dimensions of climate change correlated with endophytes' temporal re-  
523 sponses, however we do not know why trends in prevalence were weak in some areas or how  
524 endophytes would respond to more extreme changes in climate. The "time machine" of natu-  
525 ral history collections revealed evidence of mutualism resilience for grass-endophyte symbioses  
526 in the face of environmental change, but more extreme changes could potentially push one or  
527 both partners beyond their physiological limits, leading to the collapse of the mutualism; more  
528 research is needed to understand what those limits might be.

529 **Acknowledgments**

530 We thank Dr. Jessica Budke for help in drafting our initial destructive sampling plan, and to the  
531 many staff members of herbaria who facilitated our research visits, as well as to the hundreds  
532 of collectors who contributed to the natural history collections. Several high schooler and un-  
533 dergraduate researchers contributed to data collection, including A. Appio-Riley, P. Bilderback,  
534 E. Chong, K. Dickens, L. Dufresne, B. Gutierrez, A. Johnson, S. Linder, E. Scales, B. Scherick,  
535 K. Schrader, E. Segal , G. Singla, and M. Tucker. This research was supported by funding from  
536 National Science Foundation (grants 1754468 and 2208857) and by funding from the Texas Ecolab  
537 Program.

538 **Statement of Authorship**

539 J.C.F. contributed to research conception, data collection, data analysis, and led manuscript draft-  
540 ing. J.M. contributed to data analysis and manuscript revisions. T.E.X.M. contributed to research  
541 conception, data collection, data analysis, and manuscript revisions.

542 **Data and Code Availability**

543 Data from this publication can be found through a publicly available repository  
544 (<https://doi.org/10.5061/dryad.rn8pk0pn0>). Code for analyses can be found through a pub-  
545 licly available repository (<https://github.com/joshuacfowler/EndoHerbarium>) that will be per-  
546 manently archived upon publication.

547

## Literature Cited

548 Michelle E Afkhami. Fungal endophyte–grass symbioses are rare in the California floristic  
549 province and other regions with mediterranean-influenced climates. *Fungal ecology*, 5(3):345–  
550 352, 2012.

551 Michelle E Afkhami and Jennifer A Rudgers. Symbiosis lost: imperfect vertical transmission of  
552 fungal endophytes in grasses. *The American Naturalist*, 172(3):405–416, 2008.

553 Michelle E Afkhami, Patrick J McIntyre, and Sharon Y Strauss. Mutualist-mediated effects on  
554 species' range limits across large geographic scales. *Ecology letters*, 17(10):1265–1273, 2014.

555 Sally N Aitken, Sam Yeaman, Jason A Holliday, Tongli Wang, and Sierra Curtis-McLane. Adap-  
556 tation, migration or extirpation: climate change outcomes for tree populations. *Evolutionary  
557 applications*, 1(1):95–111, 2008.

558 Clare E Aslan, Erika S Zavaleta, Bernie Tershy, and Donald Croll. Mutualism disruption threatens  
559 global plant biodiversity: a systematic review. *PLoS one*, 8(6):e66993, 2013.

560 Fabian E Bachl, Finn Lindgren, David L Borchers, and Janine B Illian. inlabru: an R package for  
561 bayesian spatial modelling from ecological survey data. *Methods in Ecology and Evolution*, 10(6):  
562 760–766, 2019.

563 Charles W Bacon and James F White. Stains, media, and procedures for analyzing endophytes.  
564 In *Biotechnology of endophytic fungi of grasses*, pages 47–56. CRC Press, 2018.

565 Haakon Bakka, Håvard Rue, Geir-Arne Fuglstad, Andrea Riebler, David Bolin, Janine Illian, Elias  
566 Krainski, Daniel Simpson, and Finn Lindgren. Spatial modeling with R-inla: A review. *Wiley  
567 Interdisciplinary Reviews: Computational Statistics*, 10(6):e1443, 2018.

568 Freek T Bakker, Vanessa C Bieker, and Michael D Martin. Herbarium collection-based plant  
569 evolutionary genetics and genomics, 2020.

570 Dawn R Bazely, John P Ball, Mark Vicari, Andrew J Tanentzap, Myrtille Bérenger, Tomo Rako-  
571 cevic, and Saewan Koh. Broad-scale geographic patterns in the distribution of vertically-  
572 transmitted, asexual endophytes in four naturally-occurring grasses in sweden. *Ecography*,  
573 30(3):367–374, 2007.

574 Julien Beguin, Sara Martino, Håvard Rue, and Steven G Cumming. Hierarchical analysis of  
575 spatially autocorrelated ecological data using integrated nested laplace approximation. *Methods*  
576 in *Ecology and Evolution*, 3(5):921–929, 2012.

577 Colette S Berg, Jason L Brown, and Jennifer J Weber. An examination of climate-driven flowering-  
578 time shifts at large spatial scales over 153 years in a common weedy annual. *American Journal*  
579 of *Botany*, 106(11):1435–1443, 2019.

580 Vanessa C Bieker, Fátima Sánchez Barreiro, Jacob A Rasmussen, Marie Brunier, Nathan Wales,  
581 and Michael D Martin. Metagenomic analysis of historical herbarium specimens reveals a  
582 postmortem microbial community. *Molecular ecology resources*, 20(5):1206–1219, 2020.

583 Jessica L Blois, Phoebe L Zarnetske, Matthew C Fitzpatrick, and Seth Finnegan. Climate change  
584 and the past, present, and future of biotic interactions. *Science*, 341(6145):499–504, 2013.

585 Michael Bradshaw, Uwe Braun, Marianne Elliott, Julia Kruse, Shu-Yan Liu, Guanxiu Guan, and  
586 Patrick Tobin. A global genetic analysis of herbarium specimens reveals the invasion dynamics  
587 of an introduced plant pathogen. *Fungal Biology*, 125(8):585–595, 2021.

588 D Brem and A Leuchtmann. Epichloë grass endophytes increase herbivore resistance in the  
589 woodland grass *brachypodium sylvaticum*. *Oecologia*, 126(4):522–530, 2001.

590 Tamara A Carleton and Solomon M Hsiang. Social and economic impacts of climate. *Science*, 353  
591 (6304):aad9837, 2016.

592 Shen Cheng, Ying-Ning Zou, Kamil Kuča, Abeer Hashem, Elsayed Fathi Abd\_Allah, and Qiang-

593 Sheng Wu. Elucidating the mechanisms underlying enhanced drought tolerance in plants  
594 mediated by arbuscular mycorrhizal fungi. *Frontiers in Microbiology*, 12:4029, 2021.

595 Keith Clay and Christopher Schardl. Evolutionary origins and ecological consequences of endo-  
596 phyte symbiosis with grasses. *the american naturalist*, 160(S4):S99–S127, 2002.

597 David G Clayton, Luisa Bernardinelli, and Cristina Montomoli. Spatial correlation in ecological  
598 analysis. *International journal of epidemiology*, 22(6):1193–1202, 1993.

599 KD Craven, PTW Hsiau, A Leuchtmann, W Hollin, and CL Schardl. Multigene phylogeny of  
600 epichloë species, fungal symbionts of grasses. *Annals of the Missouri Botanical Garden*, pages  
601 14–34, 2001.

602 Kerri M Crawford, John M Land, and Jennifer A Rudgers. Fungal endophytes of native grasses  
603 decrease insect herbivore preference and performance. *Oecologia*, 164:431–444, 2010.

604 Michael S Crossley, Timothy D Meehan, Matthew D Moran, Jeffrey Glassberg, William E Snyder,  
605 and Andrew K Davis. Opposing global change drivers counterbalance trends in breeding north  
606 american monarch butterflies. *Global change biology*, 28(15):4726–4735, 2022.

607 Christopher Daly and Kirk Bryant. The prism climate and weather system—an introduction.  
608 *Corvallis, OR: PRISM climate group*, 2, 2013.

609 Barnabas H Daru, Daniel S Park, Richard B Primack, Charles G Willis, David S Barrington,  
610 Timothy JS Whitfeld, Tristram G Seidler, Patrick W Sweeney, David R Foster, Aaron M Ellison,  
611 et al. Widespread sampling biases in herbaria revealed from large-scale digitization. *New  
612 Phytologist*, 217(2):939–955, 2018.

613 Barnabas H Daru, Elizabeth A Bowman, Donald H Pfister, and A Elizabeth Arnold. A novel proof  
614 of concept for capturing the diversity of endophytic fungi preserved in herbarium specimens.  
615 *Philosophical Transactions of the Royal Society B*, 374(1763):20170395, 2019.

616 Charles C Davis, Charles G Willis, Bryan Connolly, Courtland Kelly, and Aaron M Ellison.  
617 Herbarium records are reliable sources of phenological change driven by climate and pro-  
618 vide novel insights into species' phenological cueing mechanisms. *American journal of botany*,  
619 102(10):1599–1609, 2015.

620 Andrew J Davitt, Marcus Stansberry, and Jennifer A Rudgers. Do the costs and benefits of fungal  
621 endophyte symbiosis vary with light availability? *New Phytologist*, 188(3):824–834, 2010.

622 Andrew J Davitt, Chris Chen, and Jennifer A Rudgers. Understanding context-dependency in  
623 plant–microbe symbiosis: the influence of abiotic and biotic contexts on host fitness and the  
624 rate of symbiont transmission. *Environmental and Experimental Botany*, 71(2):137–145, 2011.

625 Facundo A Decunta, Luis I Pérez, Dariusz P Malinowski, Marco A Molina-Montenegro, and  
626 Pedro E Gundel. A systematic review on the effects of epichloë fungal endophytes on drought  
627 tolerance in cool-season grasses. *Frontiers in plant science*, 12:644731, 2021.

628 Mauro Di Luzio, Gregory L Johnson, Christopher Daly, Jon K Eischeid, and Jeffrey G Arnold.  
629 Constructing retrospective gridded daily precipitation and temperature datasets for the con-  
630 terminous united states. *Journal of Applied Meteorology and Climatology*, 47(2):475–497, 2008.

631 Marion L Donald, Teresa F Bohner, Kory M Kolis, R Alan Shadow, Jennifer A Rudgers, and  
632 Tom EX Miller. Context-dependent variability in the population prevalence and individual  
633 fitness effects of plant–fungal symbiosis. *Journal of Ecology*, 109(2):847–859, 2021.

634 AE Douglas. Host benefit and the evolution of specialization in symbiosis. *Heredity*, 81(6):599–  
635 603, 1998.

636 Yuan-Wen Duan, Haibao Ren, Tao Li, Lin-Lin Wang, Zhi-Qiang Zhang, Yan-Li Tu, and Yong-Ping  
637 Yang. A century of pollination success revealed by herbarium specimens of seed pods. *New  
638 Phytologist*, 224(4):1512–1517, 2019.

639 Erika J Edwards, Brent D Mishler, and Charles D Davis. University herbaria are uniquely impor-  
640 tant. *Trends in Plant Science*.

641 Markus Engel, Tobias Mette, and Wolfgang Falk. Spatial species distribution models: Using  
642 bayes inference with inla and spde to improve the tree species choice for important european  
643 tree species. *Forest Ecology and Management*, 507:119983, 2022.

644 Sanne M Evers, Tiffany M Knight, David W Inouye, Tom EX Miller, Roberto Salguero-Gómez,  
645 Amy M Iler, and Aldo Compagnoni. Lagged and dormant season climate better predict plant  
646 vital rates than climate during the growing season. *Global Change Biology*, 27(9):1927–1941,  
647 2021.

648 Paul EM Fine. Vectors and vertical transmission: an epidemiologic perspective. *Annals of the New  
649 York Academy of Sciences*, 266(1):173–194, 1975.

650 Joshua C Fowler, Marion L Donald, Judith L Bronstein, and Tom EX Miller. The geographic  
651 footprint of mutualism: How mutualists influence species' range limits. *Ecological Monographs*,  
652 93(1):e1558, 2023.

653 Joshua C Fowler, Shaun Ziegler, Kenneth D Whitney, Jennifer A Rudgers, and Tom EX Miller.  
654 Microbial symbionts buffer hosts from the demographic costs of environmental stochasticity.  
655 *Ecology Letters*, 27(5):e14438, 2024.

656 PR Frade, F De Jongh, F Vermeulen, J Van Bleijswijk, and RPM Bak. Variation in symbiont  
657 distribution between closely related coral species over large depth ranges. *Molecular Ecology*,  
658 17(2):691–703, 2008.

659 Megan E Frederickson. Mutualisms are not on the verge of breakdown. *Trends in ecology &  
660 evolution*, 32(10):727–734, 2017.

661 Sarah E Gilman, Mark C Urban, Joshua Tewksbury, George W Gilchrist, and Robert D Holt. A

662 framework for community interactions under climate change. *Trends in ecology & evolution*, 25  
663 (6):325–331, 2010.

664 Gustaf Granath, Mark Vicari, Dawn R Bazely, John P Ball, Adriana Puentes, and Tomo Rakoce-  
665 vic. Variation in the abundance of fungal endophytes in fescue grasses along altitudinal and  
666 grazing gradients. *Ecography*, 30(3):422–430, 2007.

667 Andrin Gross, Célia Petitcollin, Cyril Dutech, Bayo Ly, Marie Massot, Julie Faivre d’Arcier, Laure  
668 Dubois, Gilles Saint-Jean, and Marie-Laure Desprez-Loustau. Hidden invasion and niche con-  
669 traction revealed by herbaria specimens in the fungal complex causing oak powdery mildew  
670 in europe. *Biological Invasions*, 23:885–901, 2021.

671 Edmund M. Hart and Kendon Bell. prism: Download data from the oregon prism project. 2015.  
672 doi: 10.5281/zenodo.33663. URL <https://github.com/ropensci/prism>. R package version  
673 0.0.6.

674 J Mason Heberling and David J Burke. Utilizing herbarium specimens to quantify historical  
675 mycorrhizal communities. *Applications in plant sciences*, 7(4):e01223, 2019.

676 Robert J Hijmans, Steven Phillips, John Leathwick, Jane Elith, and Maintainer Robert J Hijmans.  
677 Package ‘dismo’. *Circles*, 9(1):1–68, 2017.

678 Janneke HilleRisLambers, Melanie A Harsch, Ailene K Ettinger, Kevin R Ford, and Elinore J  
679 Theobald. How will biotic interactions influence climate change–induced range shifts? *Annals  
680 of the New York Academy of Sciences*, 1297(1):112–125, 2013.

681 IPCC. Climate change 2021: The physical science basis, 2021. URL  
682 <https://www.ipcc.ch/report/ar6/wg1/>.

683 Nick JB Isaac, Marta A Jarzyna, Petr Keil, Lea I Dambly, Philipp H Boersch-Supan, Ella Browning,  
684 Stephen N Freeman, Nick Golding, Gurutzeta Guillera-Arroita, Peter A Henrys, et al. Data

685 integration for large-scale models of species distributions. *Trends in ecology & evolution*, 35(1):  
686 56–67, 2020.

687 Alberto Jiménez-Valverde. Insights into the area under the receiver operating characteristic curve  
688 (auc) as a discrimination measure in species distribution modelling. *Global Ecology and Biogeog-*  
689 *raphy*, 21(4):498–507, 2012.

690 David Kahle, Hadley Wickham, and Maintainer David Kahle. Package ‘ggmap’. *Retrieved Septem-*  
691 *ber*, 5:2021, 2019.

692 Melanie R Kazenel, Catherine L Debban, Luciana Ranelli, Will Q Hendricks, Y Anny Chung,  
693 Thomas H Pendergast IV, Nikki D Charlton, Carolyn A Young, and Jennifer A Rudgers. A  
694 mutualistic endophyte alters the niche dimensions of its host plant. *AoB plants*, 7:plv005, 2015.

695 Roland A Knapp, Gary M Fellers, Patrick M Kleeman, David AW Miller, Vance T Vredenburg,  
696 Erica Bree Rosenblum, and Cheryl J Briggs. Large-scale recovery of an endangered amphibian  
697 despite ongoing exposure to multiple stressors. *Proceedings of the National Academy of Sciences*,  
698 113(42):11889–11894, 2016.

699 Mikhail V Kozlov, Irina V Sokolova, Vitali Zverev, Alexander A Egorov, Mikhail Y Goncharov,  
700 and Elena L Zvereva. Biases in estimation of insect herbivory from herbarium specimens.  
701 *Scientific Reports*, 10(1):12298, 2020.

702 Benjamin R Lee, Evelyn F Alecrim, Tara K Miller, Jessica RK Forrest, J Mason Heberling,  
703 Richard B Primack, and Risa D Sargent. Phenological mismatch between trees and wildflow-  
704 ers: Reconciling divergent findings in two recent analyses. *Journal of Ecology*, 112(6):1184–1199,  
705 2024.

706 James Lendemer, Barbara Thiers, Anna K Monfils, Jennifer Zaspel, Elizabeth R Ellwood, Andrew  
707 Bentley, Katherine LeVan, John Bates, David Jennings, Dori Contreras, et al. The extended  
708 specimen network: A strategy to enhance us biodiversity collections, promote research and  
709 education. *BioScience*, 70(1):23–30, 2020.

710 711 A Leuchtmann. Systematics, distribution, and host specificity of grass endophytes. *Natural toxins*,  
1(3):150–162, 1992.

712 713 714 Adrian Leuchtmann, Charles W Bacon, Christopher L Schardl, James F White Jr, and Mariusz  
Tadych. Nomenclatural realignment of neotyphodium species with genus epichloë. *Mycologia*,  
106(2):202–215, 2014.

715 716 717 Finn Lindgren, Håvard Rue, and Johan Lindström. An explicit link between gaussian fields and  
gaussian markov random fields: the stochastic partial differential equation approach. *Journal  
of the Royal Statistical Society: Series B (Statistical Methodology)*, 73(4):423–498, 2011.

718 719 Canran Liu, Pam M Berry, Terence P Dawson, and Richard G Pearson. Selecting thresholds of  
occurrence in the prediction of species distributions. *Ecography*, 28(3):385–393, 2005.

720 721 722 723 Margaret McFall-Ngai, Michael G Hadfield, Thomas CG Bosch, Hannah V Carey, Tomislav  
Domazet-Lošo, Angela E Douglas, Nicole Dubilier, Gerard Eberl, Tadashi Fukami, Scott F  
Gilbert, et al. Animals in a bacterial world, a new imperative for the life sciences. *Proceedings  
of the National Academy of Sciences*, 110(9):3229–3236, 2013.

724 725 726 Timothy D Meehan, Nicole L Michel, and Håvard Rue. Spatial modeling of audubon christmas  
bird counts reveals fine-scale patterns and drivers of relative abundance trends. *Ecosphere*, 10  
(4):e02707, 2019.

727 728 Emily K Meineke, Charles C Davis, and T Jonathan Davies. The unrealized potential of herbaria  
for global change biology. *Ecological Monographs*, 88(4):505–525, 2018.

729 730 731 Emily K Meineke, Aimée T Classen, Nathan J Sanders, and T Jonathan Davies. Herbarium  
specimens reveal increasing herbivory over the past century. *Journal of Ecology*, 107(1):105–117,  
2019.

732 Abigail R Meyer, Maria Valentin, Laima Liulevicius, Tami R McDonald, Matthew P Nelsen, Jean

733 Pengra, Robert J Smith, and Daniel Stanton. Climate warming causes photobiont degradation  
734 and c starvation in a boreal climate sentinel lichen. *American Journal of Botany*, 2022.

735 David AW Miller, Krishna Pacifici, Jamie S Sanderlin, and Brian J Reich. The recent past and  
736 promising future for data integration methods to estimate species' distributions. *Methods in*  
737 *Ecology and Evolution*, 10(1):22–37, 2019.

738 Daniel S Park, Ian Breckheimer, Alex C Williams, Edith Law, Aaron M Ellison, and Charles C  
739 Davis. Herbarium specimens reveal substantial and unexpected variation in phenological sen-  
740 sitivity across the eastern united states. *Philosophical Transactions of the Royal Society B*, 374  
741 (1763):20170394, 2019.

742 Martin Parniske. Arbuscular mycorrhiza: the mother of plant root endosymbioses. *Nature Reviews*  
743 *Microbiology*, 6(10):763–775, 2008.

744 Anton Pauw and Julie A Hawkins. Reconstruction of historical pollination rates reveals linked  
745 declines of pollinators and plants. *Oikos*, 120(3):344–349, 2011.

746 Shilong Piao, Qiang Liu, Anping Chen, Ivan A Janssens, Yongshuo Fu, Junhu Dai, Lingli Liu,  
747 XU Lian, Miaogen Shen, and Xiaolin Zhu. Plant phenology and global climate change: Current  
748 progresses and challenges. *Global change biology*, 25(6):1922–1940, 2019.

749 Timothée Poisot, Gabriel Bergeron, Kevin Cazelles, Tad Dallas, Dominique Gravel, Andrew Mac-  
750 Donald, Benjamin Mercier, Clément Violet, and Steve Vissault. Global knowledge gaps in  
751 species interaction networks data. *Journal of Biogeography*, 48(7):1552–1563, 2021.

752 Nicole E Rafferty, Paul J CaraDonna, and Judith L Bronstein. Phenological shifts and the fate of  
753 mutualisms. *Oikos*, 124(1):14–21, 2015.

754 Christopher J Raxworthy and Brian Tilston Smith. Mining museums for historical dna: advances  
755 and challenges in museomics. *Trends in Ecology & Evolution*, 36(11):1049–1060, 2021.

756 François Renoz, Inès Pons, and Thierry Hance. Evolutionary responses of mutualistic insect–  
757 bacterial symbioses in a world of fluctuating temperatures. *Current opinion in insect science*, 35:  
758 20–26, 2019.

759 Elizabeth Lewis Roberts and Aileen Ferraro. Rhizosphere microbiome selection by epichloë en-  
760 dophytes of *festuca arundinacea*. *Plant and soil*, 396:229–239, 2015.

761 RJ Rodriguez, JF White Jr, Anne E Arnold, and a RS and Redman. Fungal endophytes: diversity  
762 and functional roles. *New phytologist*, 182(2):314–330, 2009.

763 Gregor Rolshausen, Francesco Dal Grande, Anna D Sadowska-Deś, Jürgen Otte, and Imke  
764 Schmitt. Quantifying the climatic niche of symbiont partners in a lichen symbiosis indicates  
765 mutualist-mediated niche expansions. *Ecography*, 41(8):1380–1392, 2018.

766 Jennifer A Rudgers and Angela L Swafford. Benefits of a fungal endophyte in *elymus virginicus*  
767 decline under drought stress. *Basic and Applied Ecology*, 10(1):43–51, 2009.

768 Jennifer A Rudgers, Michelle E Afkhami, Megan A Rúa, Andrew J Davitt, Samantha Hammer,  
769 and Valérie M Huguet. A fungus among us: broad patterns of endophyte distribution in the  
770 grasses. *Ecology*, 90(6):1531–1539, 2009.

771 Jennifer A Rudgers, Rebecca A Fletcher, Eric Olivas, Carolyn A Young, Nikki D Charlton, Dean E  
772 Pearson, and John L Maron. Long-term ungulate exclusion reduces fungal symbiont prevalence  
773 in native grasslands. *Oecologia*, 181:1151–1161, 2016.

774 Håvard Rue, Sara Martino, and Nicolas Chopin. Approximate bayesian inference for latent gaus-  
775 sian models by using integrated nested laplace approximations. *Journal of the royal statistical  
776 society: Series b (statistical methodology)*, 71(2):319–392, 2009.

777 Kari Saikkonen, Pedro E Gundel, and Marjo Helander. Chemical ecology mediated by fungal  
778 endophytes in grasses. *Journal of chemical ecology*, 39:962–968, 2013.

779 Christopher L Schardl, Carolyn A Young, Jerome R Faulkner, Simona Florea, and Juan Pan.

780 Chemotypic diversity of epichloae, fungal symbionts of grasses. *fungal ecology*, 5(3):331–344,

781 2012.

782 María Semmartin, Marina Omacini, Pedro E Gundel, and Ignacio M Hernández-Agramonte.

783 Broad-scale variation of fungal-endophyte incidence in temperate grasses. *Journal of Ecology*,

784 103(1):184–190, 2015.

785 Michelle E Sneck, Jennifer A Rudgers, Carolyn A Young, and Tom EX Miller. Variation in the

786 prevalence and transmission of heritable symbionts across host populations in heterogeneous

787 environments. *Microbial Ecology*, 74:640–653, 2017.

788 Thomas F Stocker, Dahe Qin, G-K Plattner, Lisa V Alexander, Simon K Allen, Nathaniel L Bindoff,

789 F-M Bréon, John A Church, Ulrich Cubasch, Seita Emori, et al. Technical summary. In *Climate*

790 *change 2013: the physical science basis. Contribution of Working Group I to the Fifth Assessment*

791 *Report of the Intergovernmental Panel on Climate Change*, pages 33–115. Cambridge University

792 Press, 2013.

793 Peter A Stott, Nathan P Gillett, Gabriele C Hegerl, David J Karoly, Dáithí A Stone, Xuebin Zhang,

794 and Francis Zwiers. Detection and attribution of climate change: a regional perspective. *Wiley*

795 *interdisciplinary reviews: climate change*, 1(2):192–211, 2010.

796 S Sully, DE Burkepile, MK Donovan, G Hodgson, and R Van Woesik. A global analysis of coral

797 bleaching over the past two decades. *Nature communications*, 10(1):1–5, 2019.

798 E Toby Kiers, Todd M Palmer, Anthony R Ives, John F Bruno, and Judith L Bronstein. Mutualisms

799 in a changing world: an evolutionary perspective. *Ecology letters*, 13(12):1459–1474, 2010.

800 Andrew T Tredennick, Giles Hooker, Stephen P Ellner, and Peter B Adler. A practical guide to

801 selecting models for exploration, inference, and prediction in ecology. *Ecology*, 102(6):e03336,

802 2021.

803 Kevin E Trenberth, John T Fasullo, and Theodore G Shepherd. Attribution of climate extreme  
804 events. *Nature climate change*, 5(8):725–730, 2015.

805 Amy M Truitt, Martin Kapun, Rupinder Kaur, and Wolfgang J Miller. Wolbachia modifies thermal  
806 preference in *drosophila melanogaster*. *Environmental microbiology*, 21(9):3259–3268, 2019.

807 Shripad D. Tuljapurkar. Population dynamics in variable environments. III. Evo-  
808 lutionary dynamics of r-selection. *Theoretical Population Biology*, 21(1):141–165,  
809 February 1982. ISSN 0040-5809. doi: 10.1016/0040-5809(82)90010-7. URL  
810 <http://www.sciencedirect.com/science/article/pii/0040580982900107>.

811 Arantxa Urdangarin, Tomás Goicoa, and María Dolores Ugarte. Evaluating recent methods to  
812 overcome spatial confounding. *Revista Matemática Complutense*, 36(2):333–360, 2023.

813 Veronika Vikuk, Carolyn A Young, Stephen T Lee, Padmaja Nagabhyru, Markus Krischke, Mar-  
814 tin J Mueller, and Jochen Krauss. Infection rates and alkaloid patterns of different grass species  
815 with systemic epichloë endophytes. *Applied and Environmental Microbiology*, 85(17):e00465–19,  
816 2019.

817 Zhengfeng Wang, Chunjie Li, and James White. Effects of epichloë endophyte infection on  
818 growth, physiological properties and seed germination of wild barley under saline conditions.  
819 *Journal of Agronomy and Crop Science*, 206(1):43–51, 2020.

820 Robert J Warren and Mark A Bradford. Mutualism fails when climate response differs between  
821 interacting species. *Global Change Biology*, 20(2):466–474, 2014.

822 Nicole S Webster, Rose E Cobb, and Andrew P Negri. Temperature thresholds for bacterial  
823 symbiosis with a sponge. *The ISME journal*, 2(8):830–842, 2008.

824 James F White and Garry T Cole. Endophyte-host associations in forage grasses. i. distribution  
825 of fungal endophytes in some species of *lolium* and *festuca*. *Mycologia*, 77(2):323–327, 1985.

826 Franziska M Willems, JF Scheepens, and Oliver Bossdorf. Forest wildflowers bloom earlier as  
827 europe warms: lessons from herbaria and spatial modelling. *New Phytologist*, 235(1):52–65,  
828 2022.

829 Charles G Willis, Elizabeth R Ellwood, Richard B Primack, Charles C Davis, Katelin D Pearson,  
830 Amanda S Gallinat, Jenn M Yost, Gil Nelson, Susan J Mazer, Natalie L Rossington, et al. Old  
831 plants, new tricks: Phenological research using herbarium specimens. *Trends in ecology &*  
832 *evolution*, 32(7):531–546, 2017.

833 Chao Xia, Nana Li, Yawen Zhang, Chunjie Li, Xingxu Zhang, and Zhibiao Nan. Role of epichloë  
834 endophytes in defense responses of cool-season grasses to pathogens: A review. *Plant disease*,  
835 102(11):2061–2073, 2018.

836 Kentaro Yoshida, Eriko Sasaki, and Sophien Kamoun. Computational analyses of ancient  
837 pathogen dna from herbarium samples: challenges and prospects. *Frontiers in plant science*,  
838 6:771, 2015.

839

## Appendix A

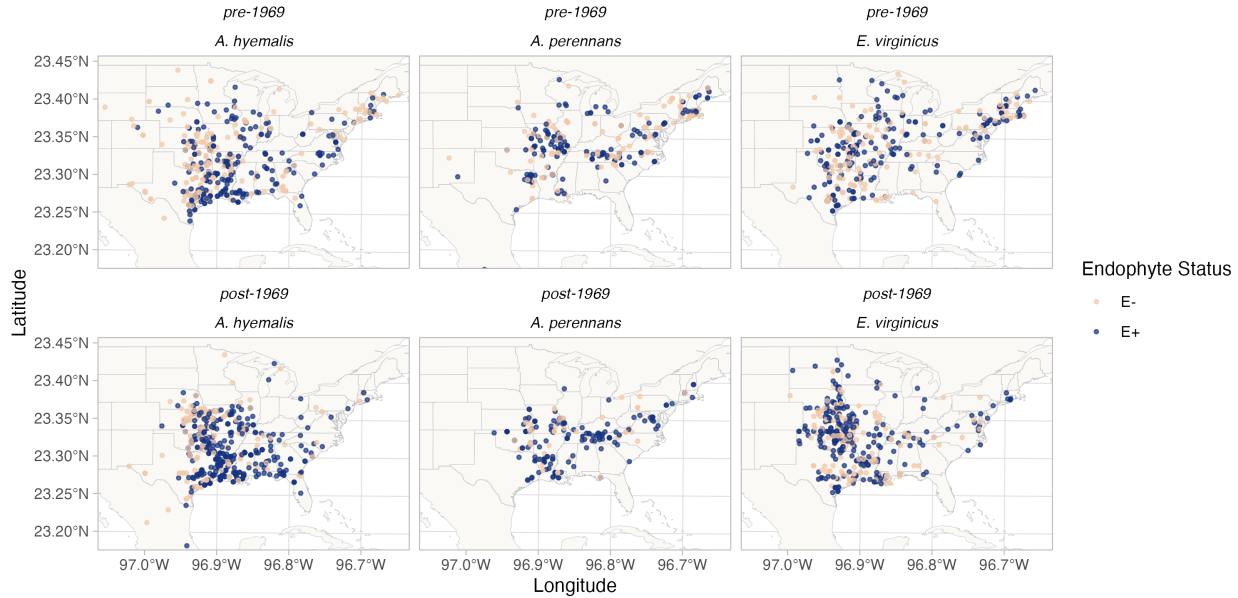


**Figure A1: Endophyte presence/absence in specimens of each host species.** Points show collection locations colored according to whether the specimen contained endophytes ( E+; blue points) or did not contain endophytes (E-, tan points). To visualize temporal change, the data are faceted before and after the median year of collection.

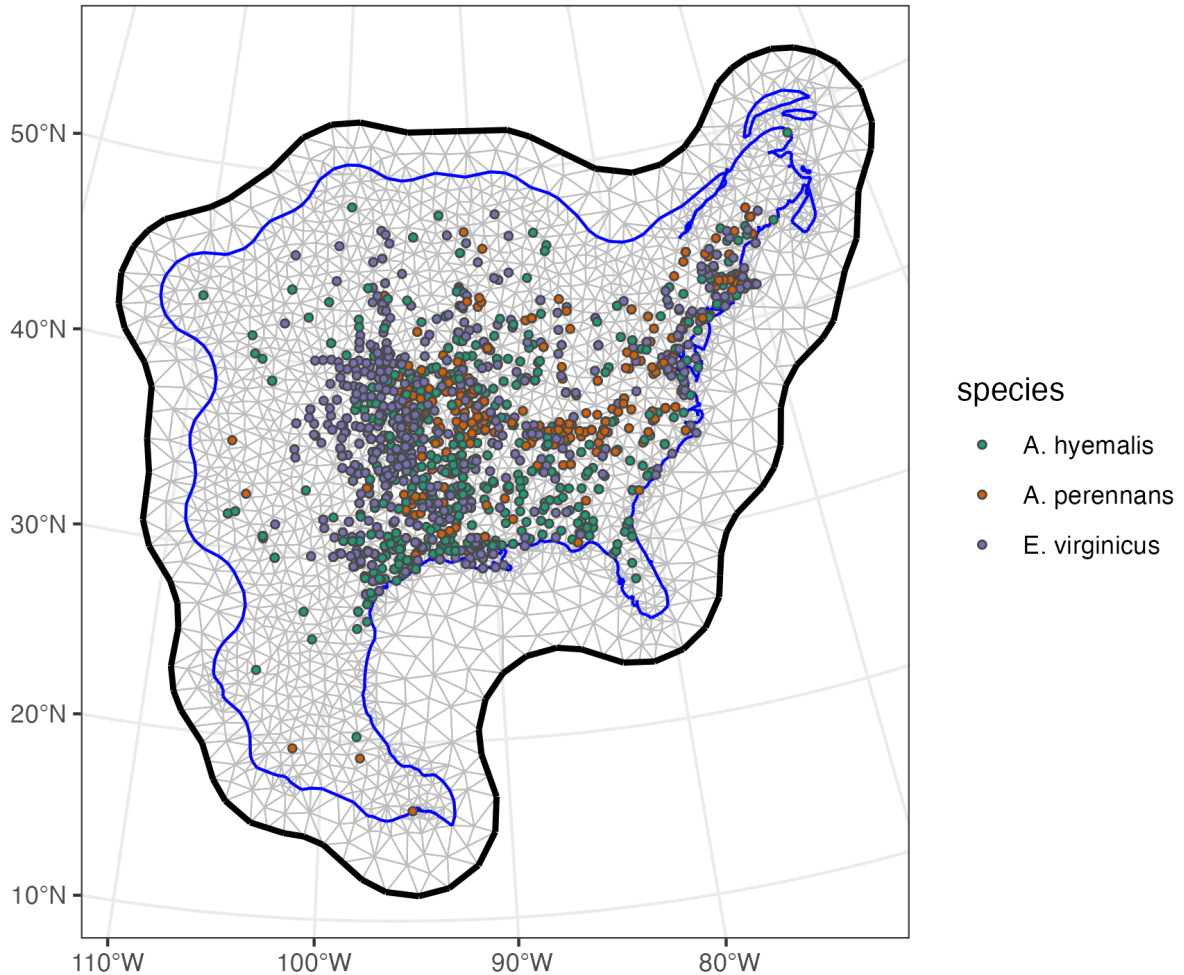


**Figure A2: Triangulation mesh used to estimate spatial dependence between data points.** Grey lines indicate edges of triangles used to define distances between observations. Colored points indicate locations of sampled herbarium specimens for each host species, and the blue line shows the convex hull and coastline used to define the edge of the mesh around the data points. The thick black line shows the convex hull defining a buffer space around the edge of the mesh to reduce the influence of edge effects on model estimates.

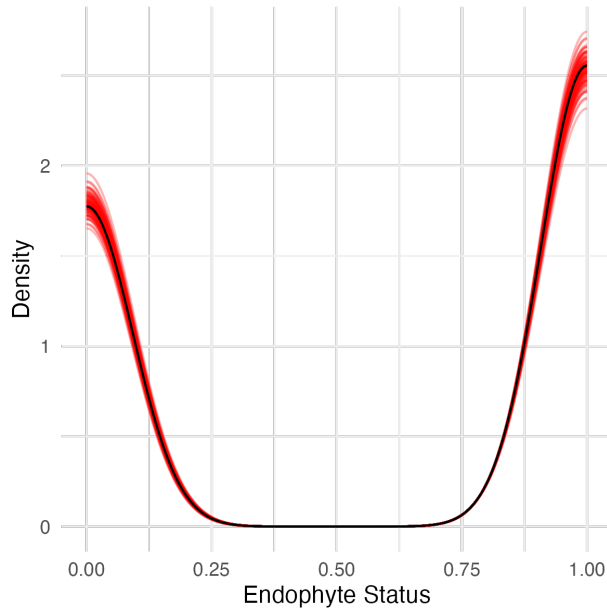


**Figure A3: Consistency between real data and simulated values indicate that the fitted model accurately describes the data.** Graph shows density curves for the observed data (black) along with 100 simulated datasets (red).

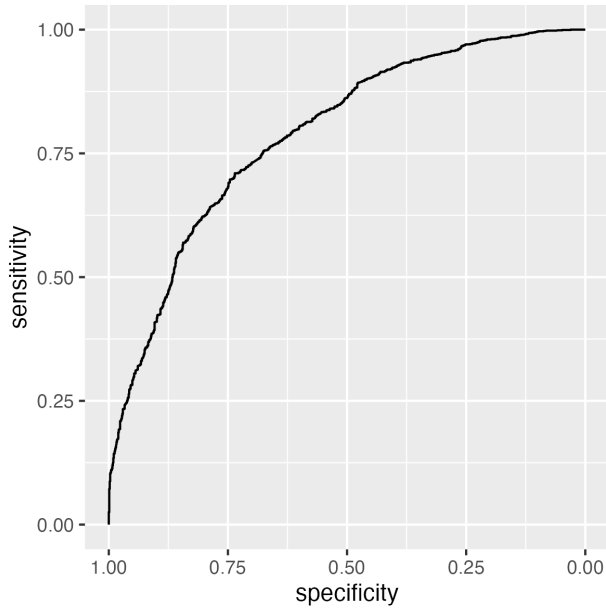


**Figure A4: ROC plot showing model performance classifying observations according to endophyte status within the in-sample data.** The curves show adequate model performance for observed data. The AUC value is 0.79.

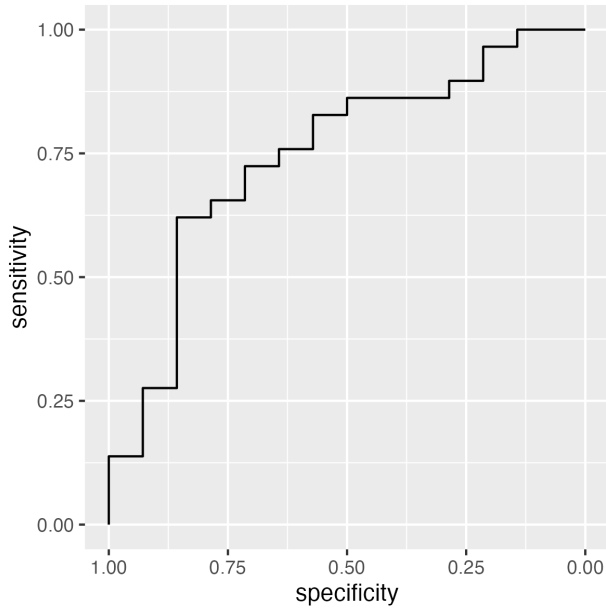


**Figure A5: ROC plot showing model performance classifying observations according to endophyte status within the out-of-sample data.** The curves show adequate model performance for test data. The AUC value is 0.77.

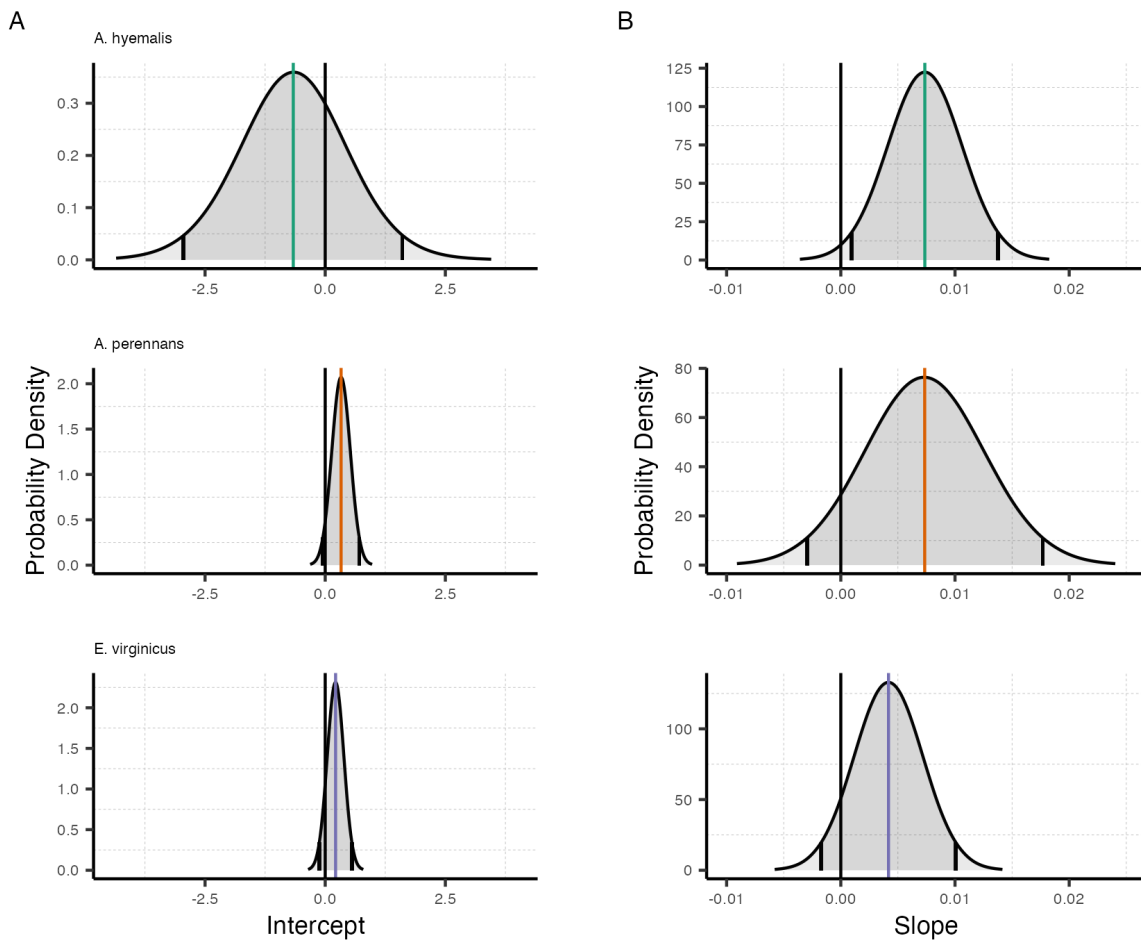


Figure A6: Density curves show the probability density along with mean (colored line) and 95% CI (black lines) for the (A) intercept and (B) slope terms, **A** and **T** respectively. Colors represent each host species

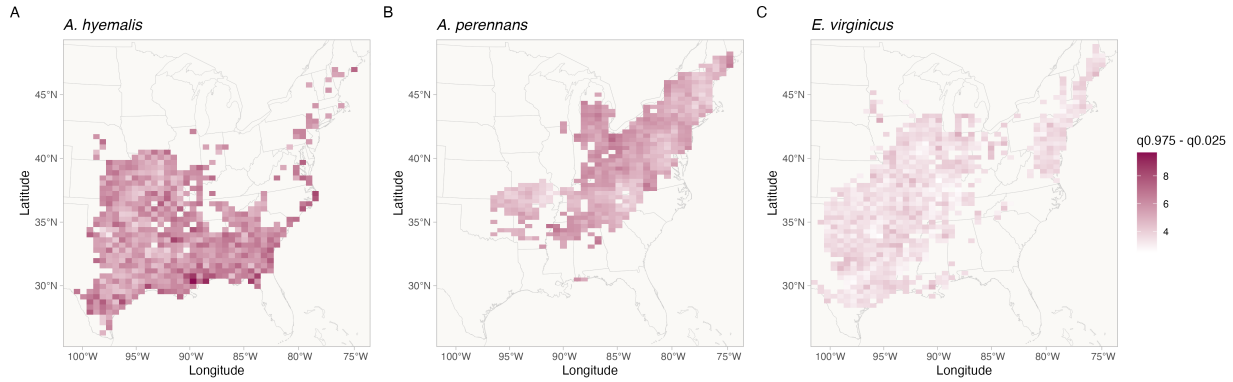


Figure A7: Shading represents the range of the 95% posterior credible interval for spatially varying slopes,  $\tau$ .

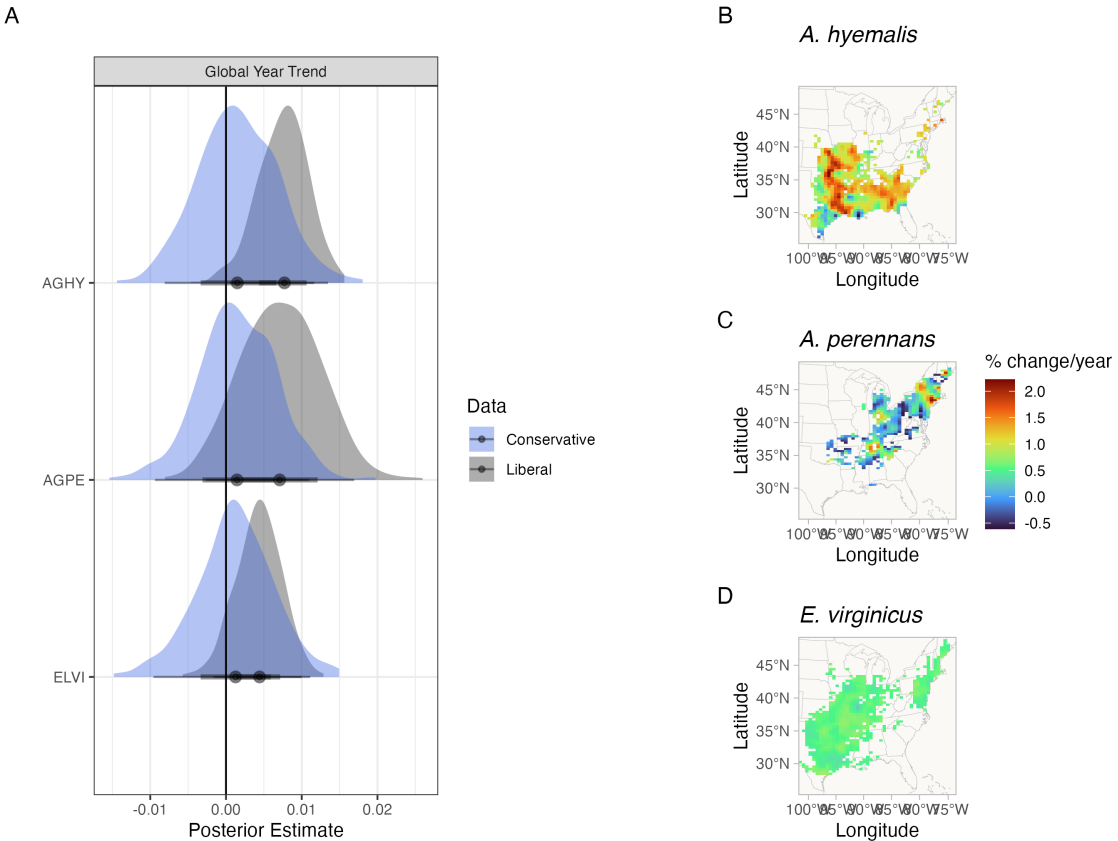


Figure A8: Comparison of liberal versus conservative endophyte scores on modeled outcomes. (A) Posterior estimates of global temporal trend for models fit to liberal scores (grey) and to conservative scores (blue). Maps show the spatially varying temporal trend estimates from model fit to conservative scores for (B) *A. hyemalis*, (C) *A. perennans*, and (D) *E. virginicus*. Note that the color scale differs between this visualization and Fig. 3.

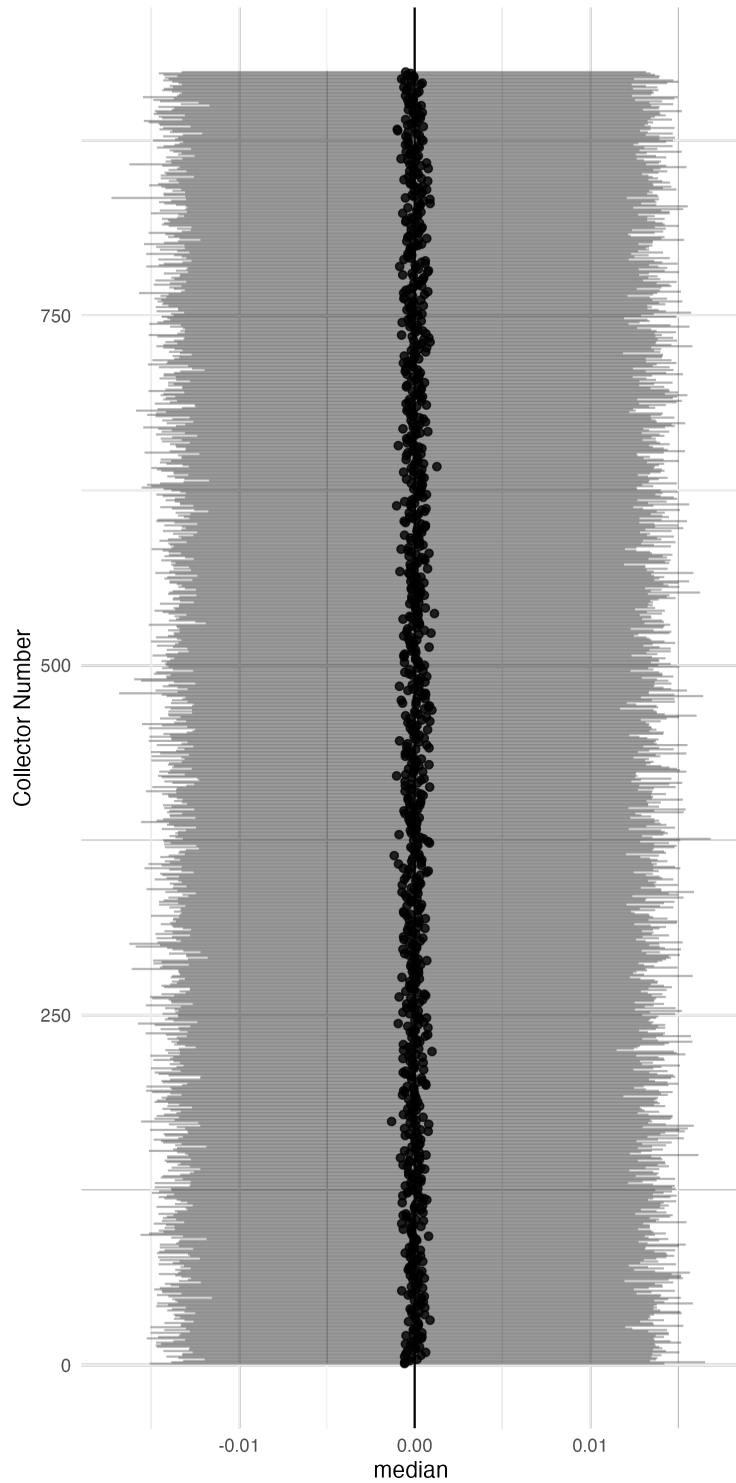


Figure A9: **Posterior estimates of collector random effects.** Points show posterior median along with 95% CI for each of 924 individual collectors.

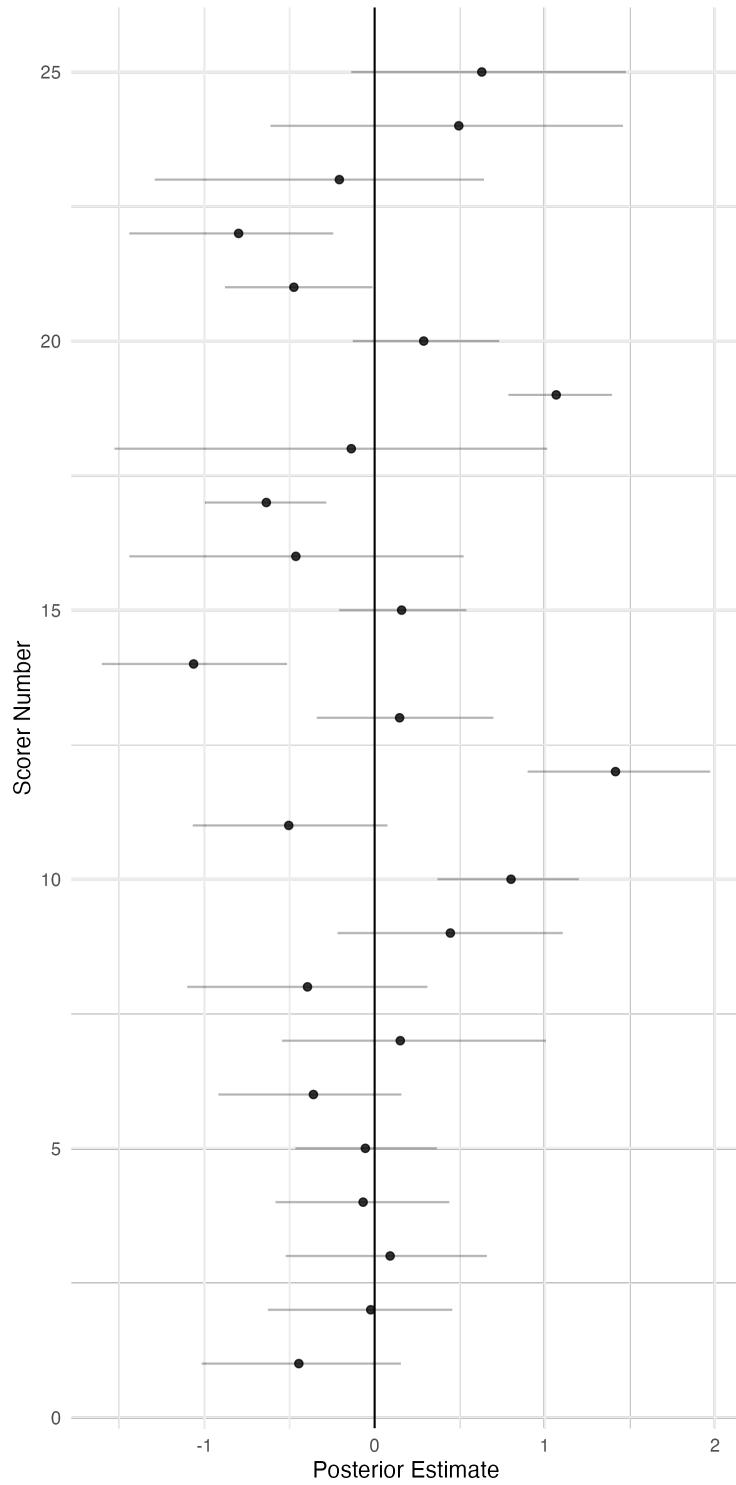


Figure A10: **Posterior estimates of scorer random effects.** Points show posterior median along with 95% CI for each of 25 individual collectors.

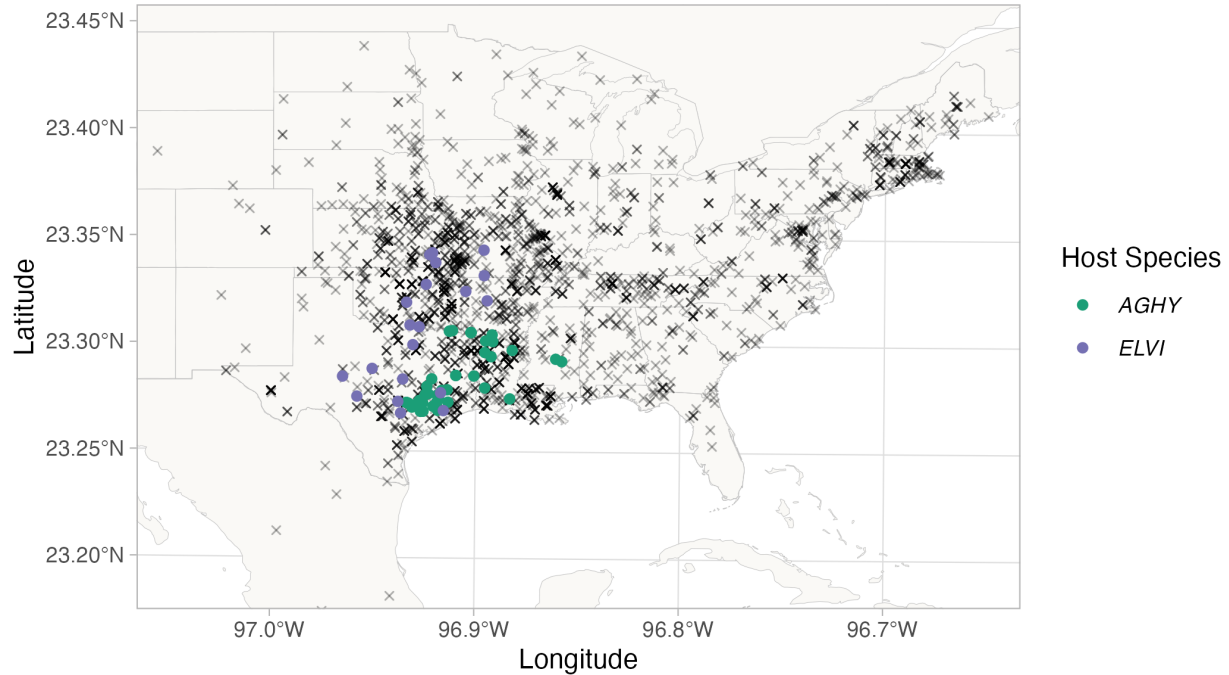
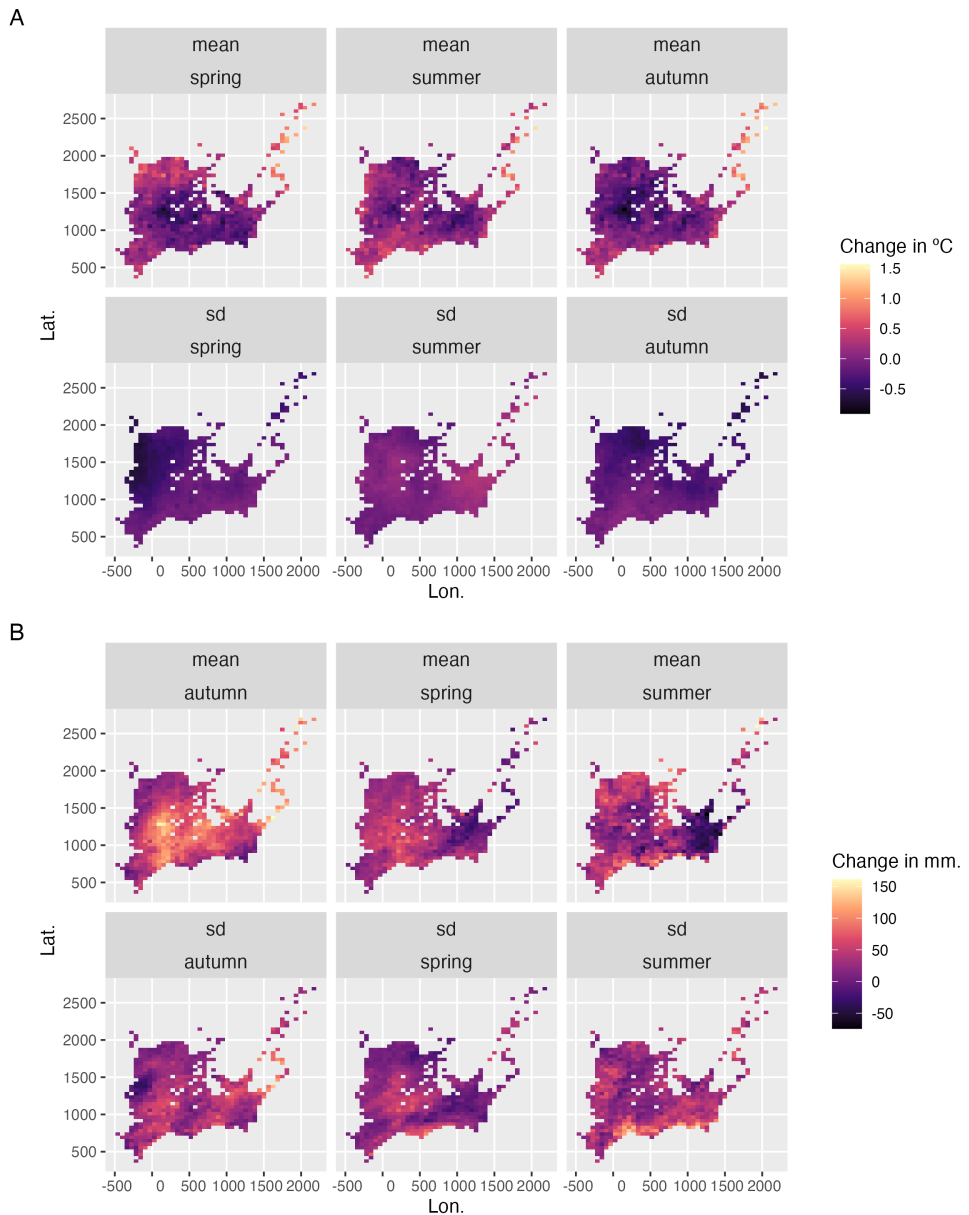
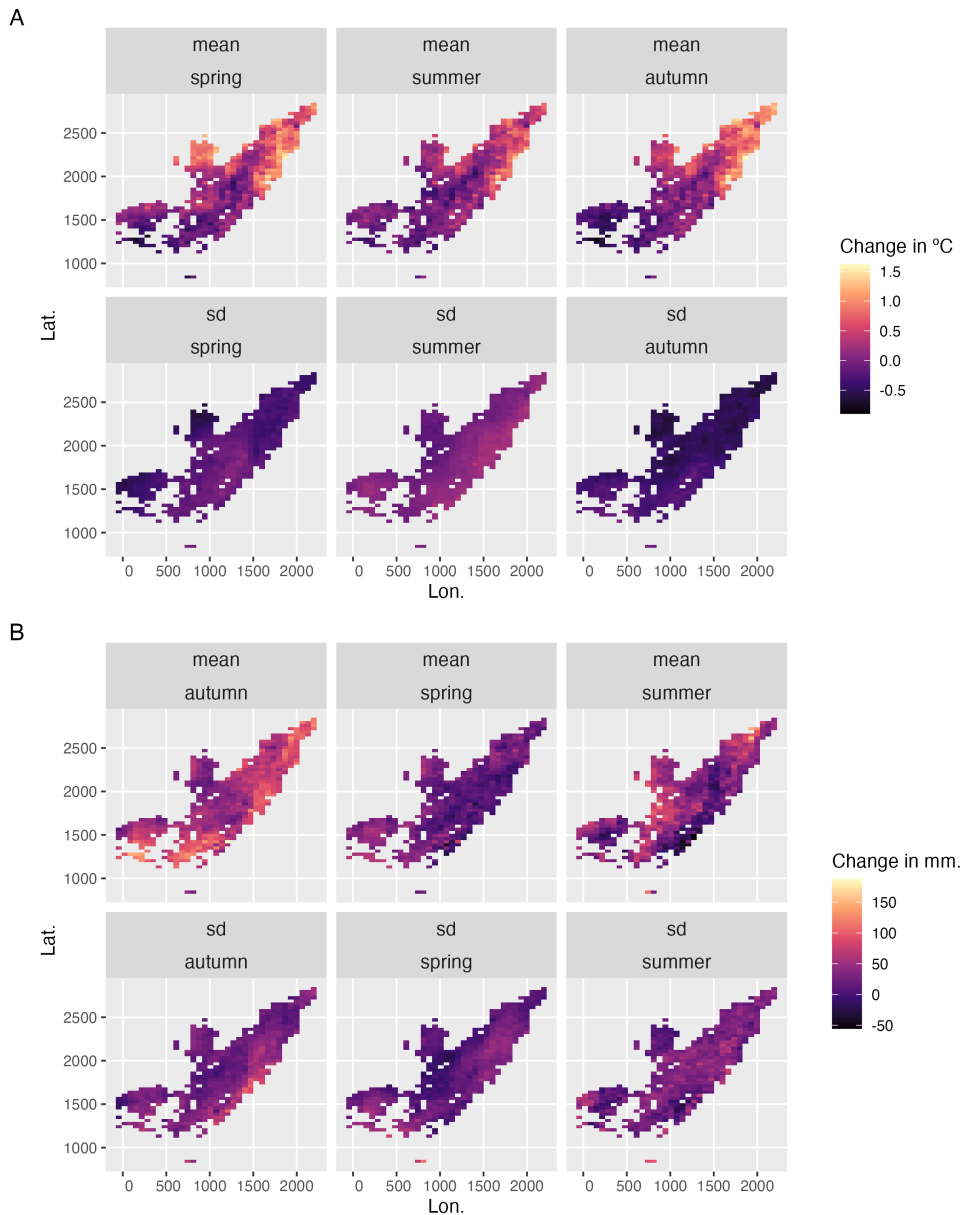


Figure A11: Locations of contemporary surveys of endophytes in *A. hyemalis* used as "test" data (red points), relative to the historical collection data (black crosses).



**Figure A12: Change in seasonal climate variables between the periods 1895-1925 and 1990-2020.** Color represents change in (A) seasonal temperature and (B) seasonal precipitation. Maps show pixels covering the modeled distribution of *A. hyemalis* used in post-hoc climate correlation analysis.



**Figure A13: Change in seasonal climate variables between the periods 1895-1925 and 1990-2020.**

Color represents change in (A) seasonal temperature and (B) seasonal precipitation. Maps show pixels covering the modeled distribution of *A. perennans* used in post-hoc climate correlation analysis.

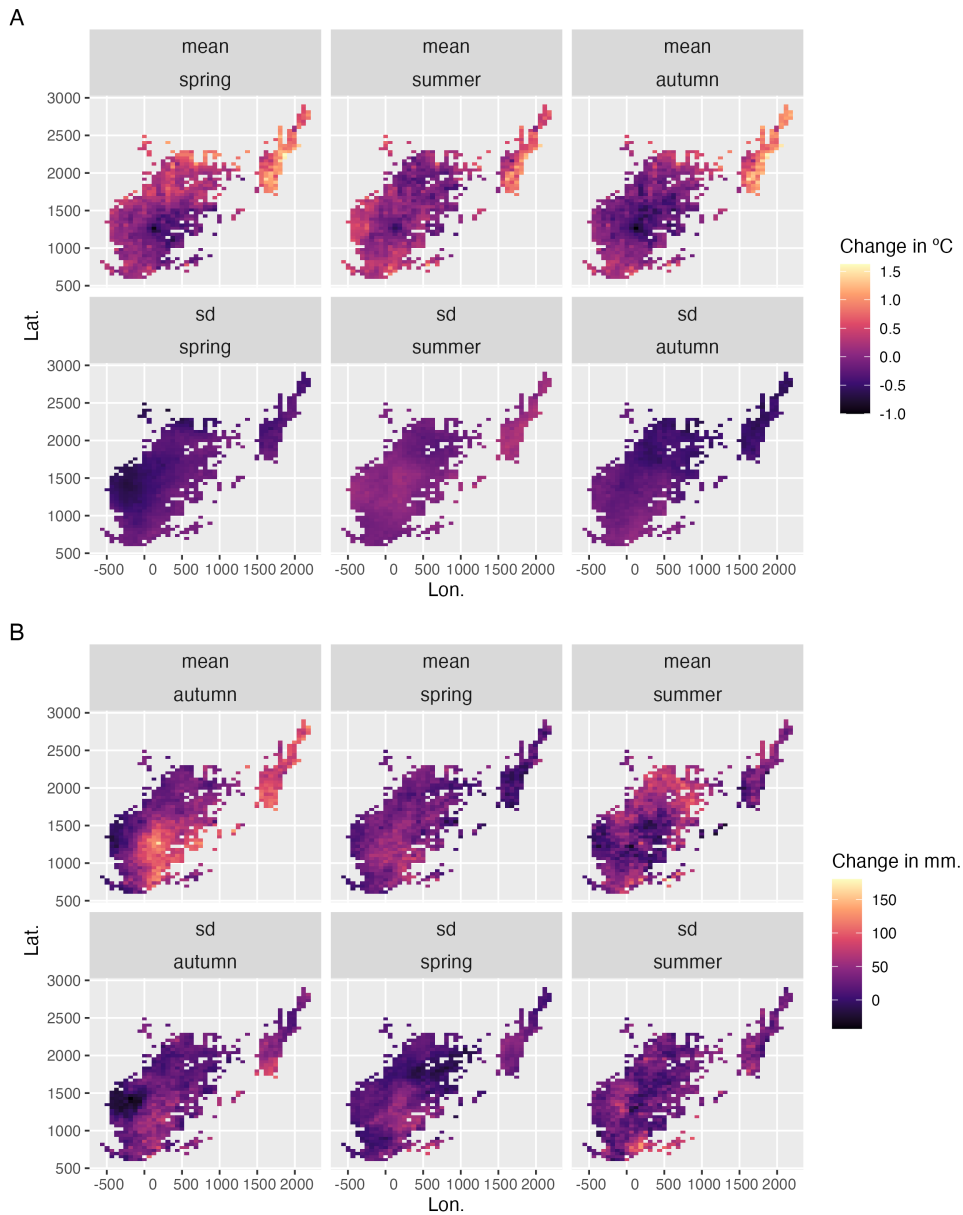


**Figure A14: Change in seasonal climate variables between the periods 1895-1925 and 1990-2020.** Color represents change in (A) seasonal temperature and (B) seasonal precipitation. Maps show pixels covering the modeled distribution of *E. virginicus* used in post-hoc climate correlation analysis.

Table A1: Summary of herbarium samples across collections

Herbarium Collection	AGHY	AGPE	ELVI
Botanical Research Institute of Texas	350	190	198
Louisiana State University	72	38	62
Mercer Botanic Garden	3	–	6
Missouri Botanic Garden	210	205	122
Texas A&M	100	–	72
University of Kansas	134	34	197
University of Oklahoma	85	34	95
University of Texas & Lundell	183	91	102
Oklahoma State University	51	10	74

840

## Supporting Methods

841

### ODMAP Protocol

#### 842 Overview

843 **Model purpose:** Mapping current distribution of *Epichloë* host species.

844 **Target species:** *Agrostis hyemalis*, *Agrostis perennans*, and *Elymus virginicus*.

845 **Study area:** Eastern North America

846 **Spatial extent:** -125.0208, -66.47917, 24.0625, 49.9375 (xmin, xmax, ymin, ymax).

847 **Spatial resolution:** 0.04166667, 0.04166667 (x, y).

848 **Temporal extent:** 1990 to 2020.

849 **Boundary:** Natural.

#### 850 Data

851 **Observation type:** Occurrence records from Global Biodiversity Information Facility and

852 herbarium collection across eastern North America. We used 713 occurrences records for

853 *Agrostis hyemalis*, 656 occurrence records for *Agrostis perennans* and 2338 for *Elymus virginicus*.

854 **Response data type:** occurrence record, presence-only.

855 **Coordinate reference system:** WGS84 coordinate reference system (EPSG:4326 code)

856 **Climatic data:** raster data extracted from PRISM

857 **Model**

858 **Model assumption:** We assumed that the target species are at equilibrium with their environment.

860 **Algorithms:** Maximum entropy (maxent)

861 **Workflow:** We described the workflow in the method section of the manuscript.

862 **Software:** All statistics were performed using Maxent 3.3.4 and R4.3.1 with packages terra, usdm, spThin and dismo.

864 **Code availability:** Available through this link: <https://github.com/joshuacfowler/EndoHerbarium>

865 **Data availability:** Will be available upon acceptance

866 **Assessment**

867 We used AUC to test model performance.

868 **Prediction**

869 We predicted the probability of presence of the host species as a binary maps (presence or  
870 absence)

## 871 *Mesh and Prior Sensitivity analysis*

872 To test the influence that the triangulation mesh and choice of priors has on results, we compared  
873 model results across a range of meshes and priors. We re-ran our model for the mesh used in  
874 main body of the text (Fig. A2), which we refer to as the "standard mesh", and with a mesh with  
875 smaller minimum vertices (finer mesh). Finer scale meshes increase computation time. For each  
876 of these meshes, we ran the model with a range of priors defining the spatial range of our spatial  
877 random effects: 342km (the prior used for presented results), as well as ranges five times smaller  
878 (68 km) and five times larger (1714 km). We found generally that these choices did not alter the

879 direction of model predictions, but did influence the associated uncertainty and magnitude of  
880 some effects.

881 For overall temporal trends, we found that models with differing priors predicted consistently  
882 positive relationships over time (Fig. A15).

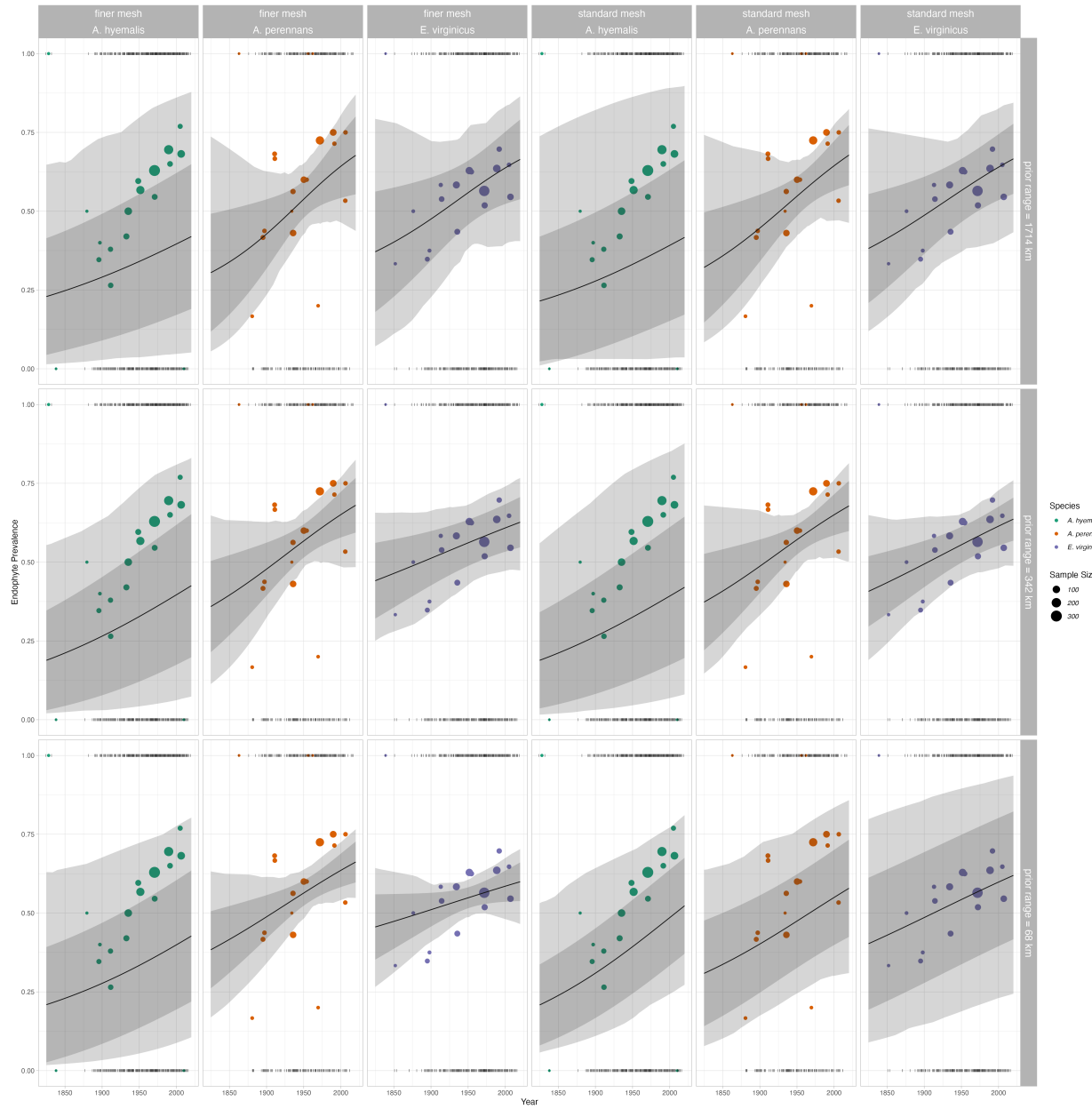


**Figure A15: Overall trend in endophyte prevalence evaluated for models with different range priors on spatially structured random effects, and for two different meshes.** Note that these plots, as compared to Fig. 2 in main text, show mean trends and do not incorporate prediction uncertainty associated with collector and scorer random effects.

883 For spatially-varying temporal trends, we found that models with different priors predicted

884 consistent spatial patterns in temporal trends, although the range of this prediction varied de-  
885 pending on the prior and mesh (Fig. A16 - A17). One noteworthy result of this analysis is that  
886 combinations of prior choice and mesh can introduce instability in model fitting. This is evident  
887 in A16 panel B and A17 panel B, where the prior range is smaller than the minimum vertex  
888 length of the mesh. Model fitting takes an extended time period and the model struggles to  
889 identify variation across space. Results with a set of prior ranges (Fig. A16 - A and C; Fig. A17  
890 - A and C) result in models that estimate trends across space of the same direction and order of  
891 magnitude, although the “smoothness” of these predictions vary.

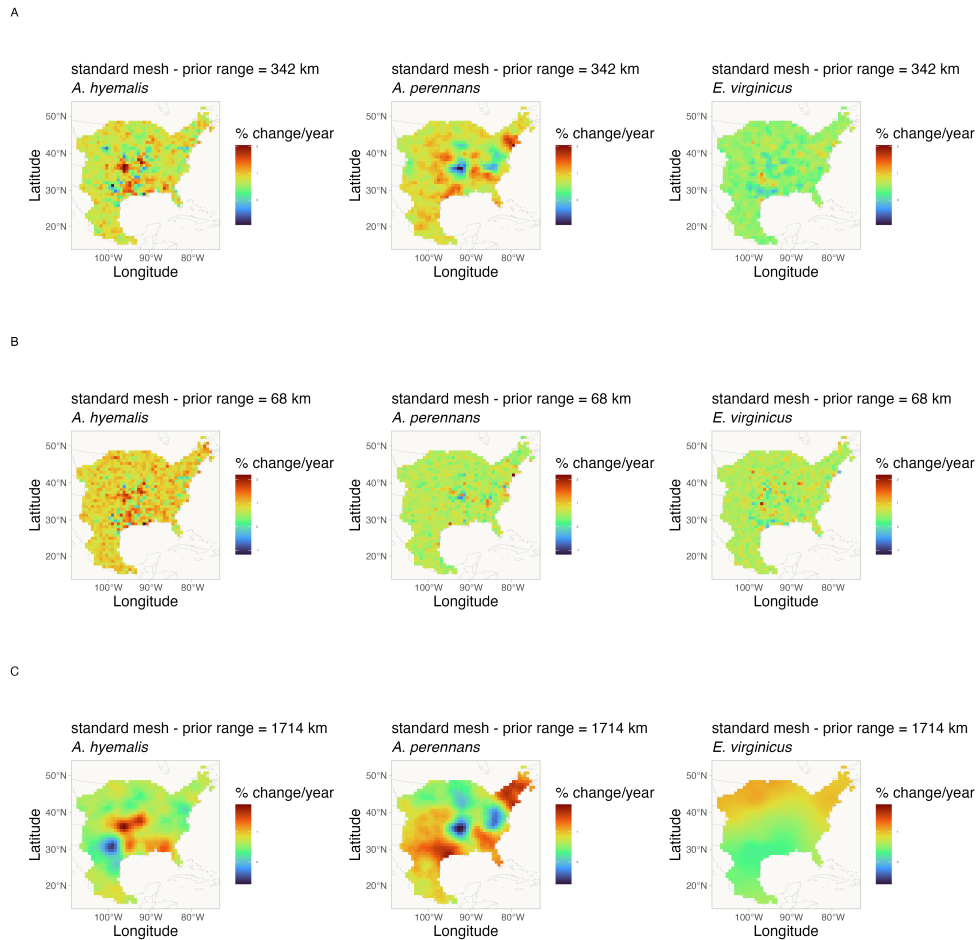


**Figure A16: Spatially-varying trends in endophyte prevalence evaluated for models with different range priors on spatially structured random effects, and for the "standard" mesh. Shading indicates the magnitude and direction of predicted trends for each of three host species for each of three prior ranges (rows A-C). Note that each plot has an individual scale bars.**

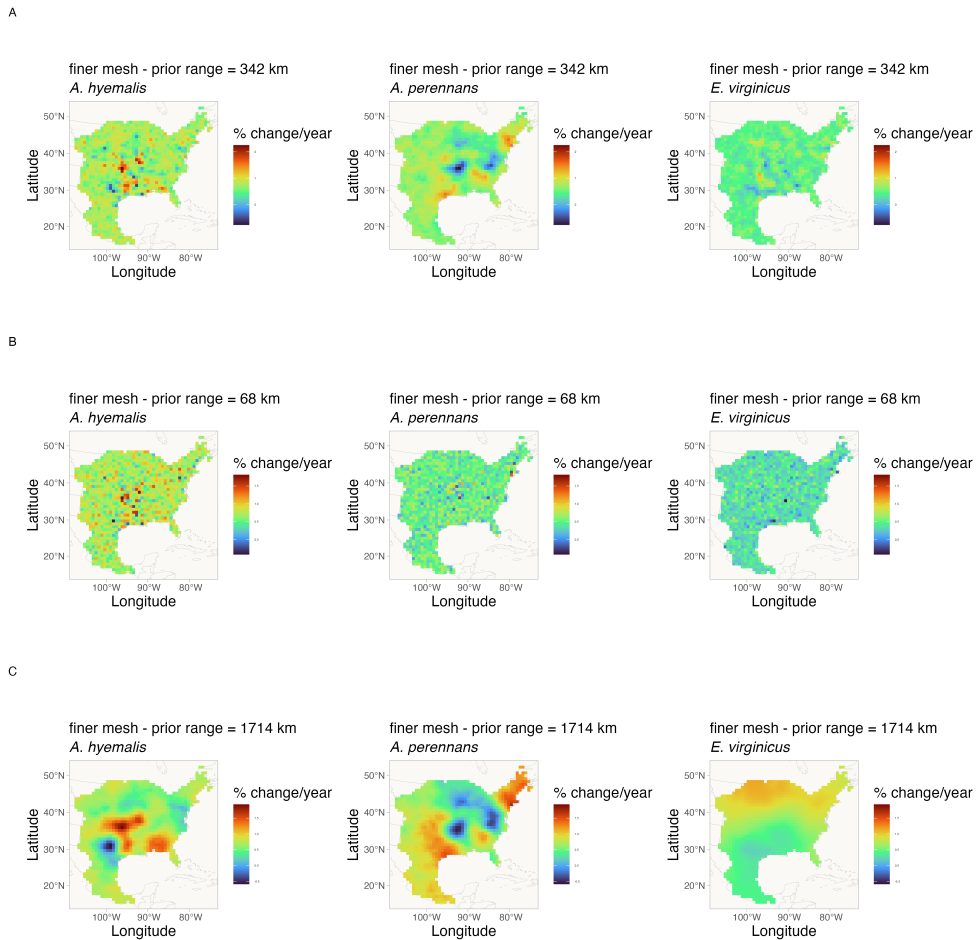


**Figure A17: Spatially-varying trends in endophyte prevalence evaluated for models with different range priors on spatially structured random effects, and for the "finer" mesh. Shading indicates the magnitude and direction of predicted trends for each of three host species for each of three prior ranges (rows A-C). Note that each plot has an individual scale bars.**